

**SELENOPROTEIN K: A STUDY INTO ITS ROLE IN ER STRESS  
MODULATION AND ERAD**

by

Osamede Owegie

A thesis submitted to the Faculty of the University of Delaware in partial fulfillment of the requirements for the degree of Master of Science in Chemistry and Biochemistry

Spring 2024

© 2024 Osamede Owegie

All Rights Reserved

**SELENOPROTEIN K: A STUDY INTO ITS ROLE IN ER STRESS  
MODULATION AND ERAD**

by

Osamede Owegie

Approved: \_\_\_\_\_  
Sharon Rozovsky, Ph.D.  
Professor in charge of thesis on behalf of the Advisory  
Committee

Approved: \_\_\_\_\_  
Joel Rosenthal, Ph.D.  
Chair of the Department of Chemistry and Biochemistry

Approved: \_\_\_\_\_  
Debra Hess Norris  
Interim Dean of the College of Arts and Sciences

Approved: \_\_\_\_\_  
Louis F. Rossi, Ph.D.  
Vice Provost for Graduate and Professional Educational  
Dean of the Graduate College

## ACKNOWLEDGEMENTS

I extend my heartfelt gratitude to my advisor, Professor Sharon Rozovsky, for her unwavering support, guidance, and mentorship throughout my academic journey. Her dedication and commitment have been instrumental in shaping and enriching my research experience. I am profoundly grateful for her thoughtful suggestions, feedback, and insights, which have deepened my understanding of my work. I also appreciate her role in fostering a collaborative and dynamic research environment that encourages intellectual exchange and growth.

Special thanks to George Woodward for his mentorship in the lab and his invaluable assistance with the purification of the selenok membrane region. I am also grateful to Atinuke Odunsi for her mentorship, feedback, and training in mammalian cell culture, which has been integral to my thesis. Additionally, I extend my appreciation to Fabio Gonzalez, Mariia Kapitonova, and Samiran Subedi for their support and engaging research discussions in the lab.

I am deeply indebted to my family for their unwavering support and encouragement throughout this journey. To my mum and siblings, your love and encouragement have been my source of strength. Lastly, I acknowledge and thank God for His boundless mercies and grace, which have sustained me.

## TABLE OF CONTENTS

LIST OF TABLES.....	vi
LIST OF FIGURES.....	vii
ABSTRACT.....	viii
Chapter	
1 INTRODUCTION.....	1
1.1 Introduction to Selenocysteine and the Human Selenoproteome.....	1
1.2 Selenoprotein k: Function and Structure.....	2
1.2.1 Function.....	2
1.2.2 Structure.....	4
1.3 Protein Homeostasis, ERAD, and the AAA+ ATPase p97: An Overview.....	6
1.4 Known Interaction Between selenoprotein K, selenoprotein S and p97 ATPase.....	8
REFERENCES.....	11
2 INVESTIGATING THE PHYSIOLOGICAL ROLE OF SELENOPROTEIN K.....	18
2.1 Background.....	18
2.2 Results.....	23
2.2.1 Cellular localization of selenoprotein k in fractionated mammalian cells.....	23
2.2.2 Identification of N-Glycosylation in Selenoprotein k.....	27
2.3 Discussion.....	29
2.4 Methods.....	30
2.4.1 Cell culture and expression of selenok constructs.....	30

2.4.2 Cellular fractionation.....	31
2.4.3 Acetone precipitation.....	31
2.4.4 Harvest and lysis.....	32
2.4.5 Measuring protein concentration.....	33
2.4.6 PNGase concentration and assay.....	33
2.4.7 Tricine SDS-PAGE gel.....	34
2.4.8 Western blotting.....	34
REFERENCES.....	36
3 PURIFICATION OF SELENOPROTEIN K AND ITS ERAD PARTNERS P97 ATPASE AND SELENOPROTEIN S.....	41
3.1 Background.....	41
3.3 Results.....	45
3.2.1 Purification of selenoprotein k (2-42 & 43-94).....	45
3.2.2 Purification of p97 ATPase.....	48
3.2.3 Purification of Selenoprotein S.....	51
3.4 Discussion.....	52
3.5 Methods.....	55
3.5.1 Expression and purification of selenok (2-43 & 43-94 U92C) selenos (1-123 U188C) and p97 (p97 His).....	55
3.5.1.1 Expression, Harvest, and Lysis.....	55
3.5.1.2 Strep-Tactin Purification:.....	57
3.5.1.3 Cation Exchange (SP) Chromatography.....	57
3.5.1.4 Size Exclusion Chromatography.....	57
3.5.2 Tricine SDS-PAGE Analysis.....	58
REFERENCES.....	59

## LIST OF TABLES

Table 2.1: The vector numbers and their corresponding selenok construct.....	30
Table 3.1: The vector numbers and their corresponding construct.....	55

## LIST OF FIGURES

Figure 1.1 Schematic diagram showing the physiological functions linked to selenok.....	4
Figure 1.2: AlphaFold2's prediction for selenok.....	6
Figure 1.3: Schematic representation of selenok and its interaction partners during ERAD.	10
Figure 2.1: Anti-selenok western blot of overexpressed HA TEV selenok 1-94 in fractioned HEK 293 cells during stress and unstressed conditions.....	26
Figure 2.2: Anti-V5 westerns of overexpressed V5 selenok U92C 1-94 at different PNGase F concentrations and incubation times at 37°C in Flp-in HEK 293 cells.....	28
Figure 3.1: AlphaFold2 prediction of Human selenok.....	44
Figure 3.2: IMAC and Strep-Tactin purification of selenok 2-42.....	46
Figure 3.3: IMAC and cation IEX (SP) chromatography purification of selenok 43-94 U92C.....	47
Figure 3.4 IMAC and SEC purification of the ATPase p97.....	49
Figure 3.5: IMAC and cation IEX (SP) chromatography purification of selenos 123-189 U188C.....	51

## **ABSTRACT**

Selenoproteins constitute a distinct protein family characterized by the incorporation of the 21st amino acid, selenocysteine (Sec or U). While some are well-characterized, there is limited in-depth knowledge on the structure and cellular roles of membrane-bound selenoprotein – one of which is selenoprotein K (selenok). Selenok is an intrinsically disordered endoplasmic reticulum (ER) membrane protein that has been reported to be upregulated during ER stress, a condition characterized by the accumulation of misfolded proteins in the ER. It has also been reported to play a role in protein quality control by associating with key players in the endoplasmic reticulum-associated protein degradation (ERAD) pathway, which retro-translocate misfolded proteins from the ER to the cytosol for proteasomal degradation. However, the specific roles of selenok in these cellular processes and pathways are not known. By employing cellular fractionation to investigate selenok's localization under different conditions, enzymatic deglycosylation to identify selenok's glycosylation, and purification of selenok and its ERAD partners, this work provides a foundation for investigating the physiological role of selenok in the ERAD pathway.

# Chapter 1

## INTRODUCTION

### 1.1 Introduction to Selenocysteine and the Human Selenoproteome

Selenoproteins constitute a distinct protein family characterized by the incorporation of the 21st amino acid, selenocysteine (Sec or U) [1]. Unlike cysteine (Cys or C), Sec differs by replacing sulfur with selenium in its chemical structure [1][2]. This unique amino acid is encoded by the opal stop codon UGA, and its insertion into proteins also requires a stable RNA structure termed the selenocysteine insertion sequence (SECIS) [2][3]. SECIS is situated in the 3'-UTR of selenoprotein mRNAs in eukaryotes and within the coding region immediately downstream of the Sec-encoding UGA codon in bacteria [3]. The SECIS, in collaboration with essential proteins like the Sec-specific eukaryotic elongation factor (eEFSEC) and SECIS binding protein 2 (SBP2), orchestrates the regulated reprogramming of UGA into Sec [1]. Beyond the intricacies of the insertion mechanism, Sec and Cys differ in their chemical reactivity. Notably, Sec exhibits a lower pKa (5.3) compared to Cys (8.3). Consequently, at the physiological pH of 7.4, Sec exists in a deprotonated state, making it a reactive nucleophile [4]. This unique property contributes to the distinctive functional aspects of selenoproteins.

Selenoprotein is ubiquitously present across the three domains of life—Eukarya, Archaea, and Bacteria [5]. Many selenoproteins function as enzymes, leveraging the reactivity of the Sec residue. Out of the 100 identified selenoprotein families, 25 are encoded in the human proteome [5] [6]. The human selenoproteome can be broadly classified based on their roles in different physiological activities. Notably, they are grouped into those that play antioxidant roles, exemplified by glutathione peroxidases and thioredoxin reductases; metabolism of thyroid hormones, as seen in deiodinases; selenium transport and storage, such as selenoprotein P; calcium metabolism, like selenoprotein K and selenoprotein T; Sec synthesis (e.g., selenophosphate synthetase 2); and protein folding (e.g., Selenoprotein N, Selenoprotein F, Selenoprotein S). However, the functions of many selenoproteins remain undefined or not well elucidated [6].

## **1.2 Selenoprotein k: Function and Structure**

### **1.2.1 Function**

Selenoprotein K, also referred to as selenok, is one of seven selenoproteins identified within the endoplasmic reticulum (ER) membrane [7]. Its expression level increases by 3-fold during ER stress; a physiological condition characterized by the accumulation of misfolded proteins within the ER lumen [8][9]. In response to ER stress, a pivotal cellular mechanism, known as endoplasmic reticulum-associated degradation (ERAD), comes into play. The ERAD is part of the protein quality control, and is responsible for detecting misfolded proteins, initiating their ubiquitination, and orchestrating their retro-translocation from the

ER to the cytosol where they are degraded [9]. Selenok has been found to be associated with key players such as Derlins and p97 ATPase in the ERAD complex [8].

Studies have shown its involvement in the palmitoylation activity of DHHC6, a palmitoyl transferase. This interaction, facilitated by SH3 interaction, stabilizes the acyl transferase and promotes palmitoylation [10]. Selenok's impact extends to the stabilization of DHHC6, emphasizing its role in protein modification and immunity. Palmitoylation is particularly important for the proper interaction and organization of membrane-associated proteins, including the inositol 1,4,5-triphosphate receptor (IP3R), a key player in store-operated calcium entry (SOCE) into immune cells [10], [11], [12]. Recent studies have also revealed selenok's involvement in vesicle formation and trafficking. Specifically, palmitoylation of CD36, which facilitates its integration into vesicles and subsequent subcellular trafficking, highlights the intricate roles of selenok in cellular processes [13].

Selenok has been implicated in signaling pathways that control growth and proliferation, as evidenced by increased apoptosis and autophagy upon its knockout or knockdown (figure 1.1) [14], [15], [16]. Reports have linked selenok to cancer progression, including melanoma and prostate cancer, underscore its potential as a regulatory element in oncogenic processes [17], [18]. Additionally, the significance of selenok in immunity is evident through its high levels in lymphoid tissues and its accumulation in lipid droplets during innate immune responses [19], [20]. However, the specific interactions in immune pathways and cancer remain elusive.

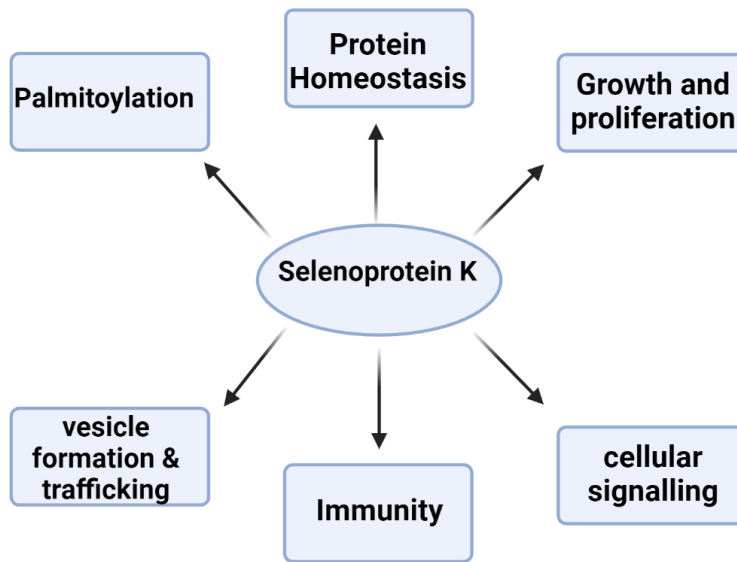


**Figure 1.1 Schematic diagram showing the physiological functions linked to selenok (created with [Biorender.com](https://www.biorender.com)).** Studies have shown selenok to participate in diverse cellular processes, including protein homeostasis, palmitoylation, immunity, cellular signaling, vesicle formation, trafficking, as well as growth and proliferation.

### 1.2.2 Structure

The structural elucidation of full-length selenoprotein K (selenok) faces challenges due to its hydrophobic nature as a membrane protein and the presence of an intrinsically disordered region (IDR), making traditional crystallization methods unlikely [21]. However, a structural model is available based on AlphaFold2 [22]. According to this prediction, selenok exhibits three distinct segments: residues 1-19 constitute the short N-terminus, residues 20-51 form a membrane-bound hydrophobic helix, and residues 51-94 comprise the intrinsically disordered C-terminus. The disordered C-terminus is rich in polar residues, prominently featuring proline and contains Sec at position 92 (Figure 1.1).

Intrinsically disordered proteins (IDPs) like selenok, often exhibit the ability to establish transient interactions with different partners to perform varied functions [23]. IDPs promiscuity is possible as they are rich in recognition features (MoRFs) or short linear motifs (SLiMs) if they are less than 10 residues [24]. Predictions from Eukaryotic Linear Motif (ELM) highlight two SH2 binding elements in selenok: one in the N-terminus (residues 3-6) and one in the disordered C-terminus (residues 60-63). Three SH3 binding sites are identified in this disordered region: residues 64-70 for class I SH3 domains, residues 67-70 for class II SH3 domains, and the third site (residues 80-86) [25].

Additionally, studies have shown that selenok are cleavage substrate for calpain proteases [26]. The webserver PROSPER which predicts proteases cleavage sites, predicts selenok to be cleaved by serine, cysteine and metalloproteases [27]. Selenok's intrinsically disordered nature, coupled with these features, implies its potential to interact with various protein partners, although only a few are currently known.

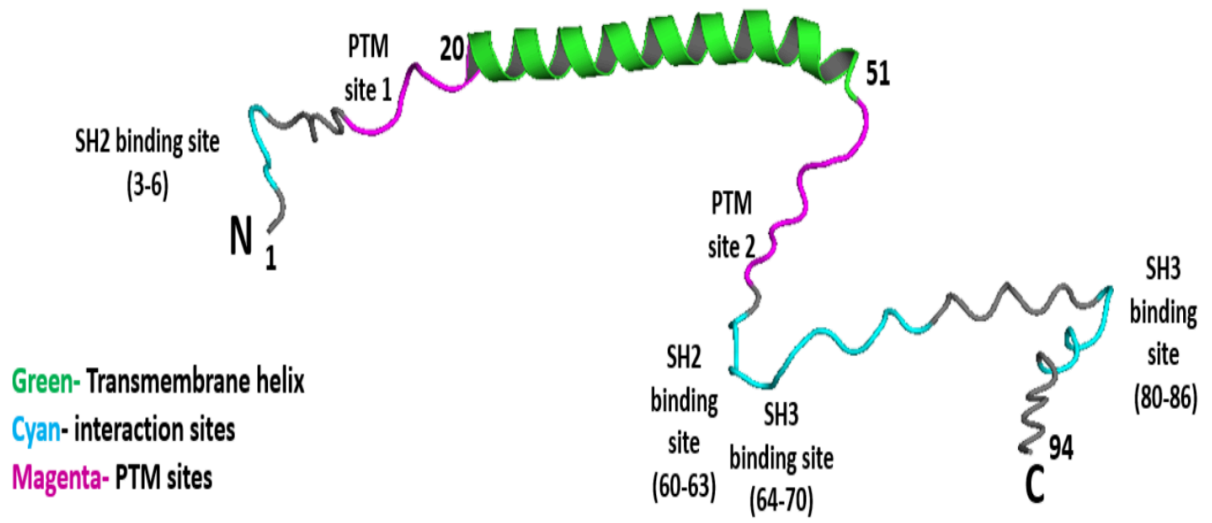


**Figure 1.2: AlphaFold2’s prediction for selenok.** AlphaFold2 predicts three distinct segments for selenok: residues 1-19 constitute the short N-terminus, residues 20-51 form a membrane-bound hydrophobic helix, and residues 51-94 comprise the intrinsically disordered C-terminus.

### 1.3 Protein Homeostasis, ERAD, and the AAA+ ATPase p97: An Overview

Proteins are central to cellular function, and their synthesis initiates in the cytosol with translation [28]. Facilitated by the signal recognition peptide (SRP) and its receptor, ribosomes laden with mRNA migrate to the ER, where proteins undergo proper folding and modifications for functionality [28], [29]. However, errors in transcription or translation, abnormal modifications, or cellular stress can lead to misfolded proteins [30]. The accumulation of misfolded proteins triggers ER stress, a condition associated with cellular dysfunction and diseases [30], [31].

To manage ER stress, cells activate the unfolded protein response (UPR) which activates the ERAD pathway [32]. As stated earlier, ERAD involves the extraction of misfolded proteins from the ER lumen into the cytosol for proteasomal degradation [32]. A crucial player in ERAD is the p97 ATPase, or valosin-containing protein (VCP), a hexameric AAA+ ATPase residing in the cytosol [33]. Structurally, p97 consists of four domains: N-terminal, D1, D2, and C-terminal, each serving distinct functions in the ERAD process. The N-terminal domain plays a crucial role in client recognition and binding, as well as binding to adapters. Simultaneously, the short C-terminus serves also as a site for adapter binding [33],[34]. The D1 and D2 domains collaboratively generate the energy required unfolding the clients [33], [34].

Derlins, which are integral membrane proteins, also contribute significantly to ERAD by forming a channel on the ER membrane [35]. The retro-translocation of misfolded proteins into the cytosol is facilitated by a channel formed by Derlins. Derlins are believed to recognize and interact with misfolded substrates, triggering the opening of a channel across the ER membrane. This interaction involves coupling with p97, utilizing its energy from ATP Hydrolysis to extract misfolded proteins from the ER into the cytosol for subsequent proteasomal degradation [35]. However, the detailed mechanism by which derlins open this channel and couple with p97 for protein extraction remains incompletely understood [36]. This process plays a vital role in maintaining ER homeostasis and preventing the harmful accumulation of misfolded proteins.

The implications of ERAD dysfunction are evident in various diseases. Accumulation of misfolded proteins is associated with neurodegenerative disorders like Alzheimer's and Parkinson's diseases, as well as other debilitating diseases, such as liver and lung diseases, and diabetes [37], [38]. Understanding how the structural domains of p97 interact with its ERAD partners like derlins provides insights into potential therapeutic targets for diseases linked to protein misfolding and ER stress.

#### **1.4 Known Interaction Between selenoprotein K, selenoprotein S and p97 ATPase**

Selenok, an ER membrane protein, shares significant parallels with Selenoprotein S (selenos), also known as VIMP, Tanis, SEPS1. Selenos is structurally predicted by AlphaFold2 [22]. It is predicted to have three  $\alpha$ -helices: Helix-1 (residues 1-33), Helix-2 (residues 34-70), and Helix-3 (residues 73-123). As a transmembrane protein, Selenos incorporates Helix-2 spanning the ER membrane, with the cytosolic segment including residues 51-123 and an IDR from residues 124-189 [39]. This IDR contains the unique Sec residue at position 188. Rich in proline, glycine, and polar charged residues, the IDRs of both selenok and selenos contribute to their functional similarity.

Both selenok and selenos are localized in the ER membrane and have established connections with key ERAD proteins, including Derlins and p97 [40]. Selenos plays a pivotal role by binding to and recruiting the p97 ATPase to the ER through a VCP interacting motif (VIM) within residues 69-108 [40], [41]. This interaction is crucial for the energy-dependent retro-translocation of misfolded proteins from the ER lumen to the

cytosol, facilitating subsequent proteasomal degradation. Although the direct interaction between selenok and p97 remains incompletely elucidated, studies suggest that Selenos recruits p97 to the ER membrane. Meanwhile, selenok interacts with the resulting complex through its association with Selenos, forming the complex (selenos-p97/VCP-selenok) that plays a vital role in ERAD and ER stress regulation [40] (Fig 1.2).

Understanding the intricacies of these interactions will provide valuable insights into the mechanisms of ERAD. Investigating how selenok and its ERAD partners contribute to the ER stress response and protein quality control can unravel new therapeutic targets for diseases associated with ER stress and misfolded proteins.

Considering the above, this thesis focuses on providing groundwork for exploring the physiological role of selenok during ER stress and ERAD.

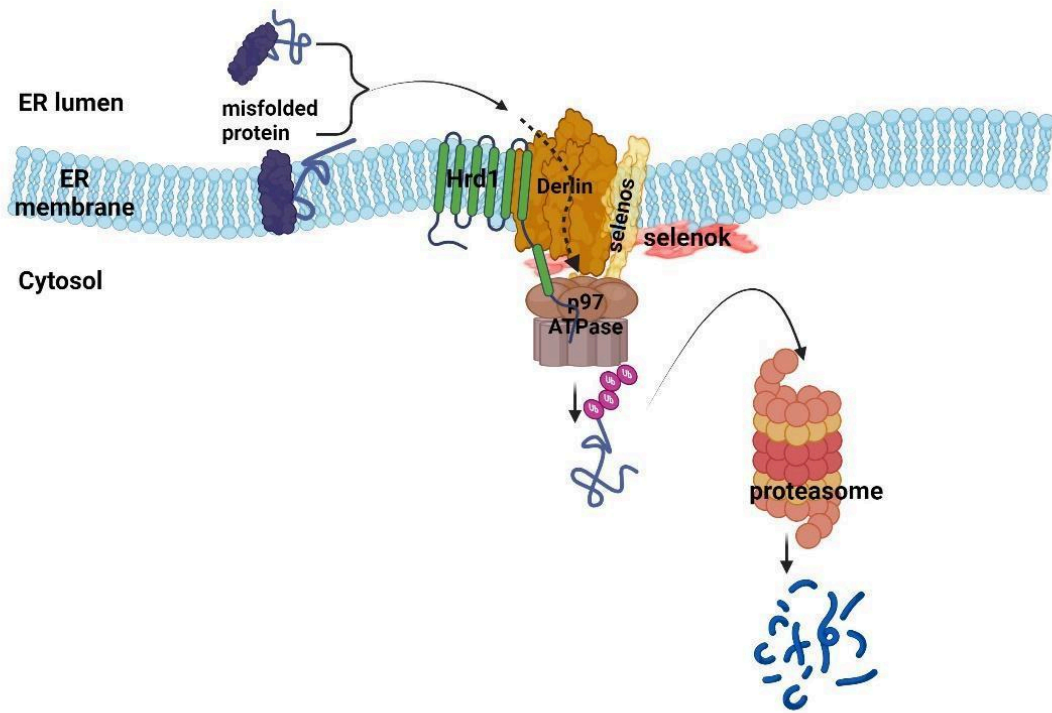


**Figure 1.3: Schematic representation of selenok and its interaction partners during ERAD (Created with [BioRender.com](https://www.biorender.com)).** Studies suggest Selenos recruits p97 to the ER membrane, while selenok interacts with the resulting complex through interaction with selenos.

## REFERENCES

- [1] D. Kang et al., “The role of selenium metabolism and selenoproteins in cartilage homeostasis and arthropathies,” *Exp Mol Med*, vol. 52, no. 8, pp. 1198–1208, Aug. 2020, doi: 10.1038/s12276-020-0408-y.
- [2] O. Vargas-Rodriguez, M. Englert, A. Merkurjev, T. Mukai, and D. Söll, “Recoding of the selenocysteine UGA codon by cysteine in the presence of a non-canonical tRNA<sup>Cys</sup> and elongation factor SelB,” *RNA Biol.*, vol. 15, no. 4–5, p. 471, May 2018, doi: 10.1080/15476286.2018.1474074.
- [3] H. Mix, A. V. Lobanov, and V. N. Gladyshev, “SECIS elements in the coding regions of selenoprotein transcripts are functional in higher eukaryotes,” *Nucleic Acids Research*, vol. 35, no. 2, pp. 414–423, Jan. 2007, doi: 10.1093/nar/gkl1060.
- [4] J. Liu and S. Rozovsky, “Membrane-Bound Selenoproteins,” *Antioxidants & Redox Signaling*, vol. 23, no. 10, pp. 795–813, Oct. 2015, doi: 10.1089/ars.2015.6388.
- [5] V. N. Gladyshev et al., “Selenoprotein Gene Nomenclature,” *Journal of Biological Chemistry*, vol. 291, no. 46, pp. 24036–24040, Nov. 2016, doi: 10.1074/jbc.M116.756155.

- [6] Reeves, M.A., Hoffmann, P.R. The human selenoproteome: recent insights into functions and regulation. *Cell. Mol. Life Sci.* 66, 2457–2478 (2009). <https://doi.org/10.1007/s00018-009-0032-4>
- [7] V. A. Shchedrina, Y. Zhang, V. M. Labunskyy, D. L. Hatfield, and V. N. Gladyshev, “Structure-function relations, physiological roles, and evolution of mammalian ER-resident selenoproteins,” *Antioxid. Redox Signal.*, vol. 12, no. 7, pp. 839–849, 2010, doi: 10.1089/ars.2009.2865
- [8] V. A. Shchedrina, R. A. Everley, Y. Zhang, S. P. Gygi, D. L. Hatfield, and V. N. Gladyshev, “Selenoprotein K Binds Multiprotein Complexes and Is Involved in the Regulation of Endoplasmic Reticulum Homeostasis \*,” *J. Biol. Chem.*, vol. 286, no. 50, pp. 42937–42948, Dec. 2011, doi: 10.1074/JBC.M111.310920
- [9] B. E. Tepedelen and P. B. Kirmizibayrak, “Endoplasmic Reticulum-Associated Degradation (ERAD),” *Endoplasmic Reticulum*, Feb. 2019, doi: 10.5772/INTECHOPEN.82043
- [10] G. J. Fredericks and P. R. Hoffmann, “Selenoprotein K and protein palmitoylation,” *Antioxid. Redox Signal.*, vol. 23, no. 10, pp. 854–862, 2015, doi: 10.1089/ars.2015.6375.
- [11] G. J. Fredericks, F. W. Hoffmann, R. J. Hondal, S. Rozovsky, J. Urschitz, and P. R. Hoffmann, “Selenoprotein K Increases Efficiency of DHHC6 Catalyzed Protein Palmitoylation by Stabilizing the Acyl-DHHC6 Intermediate,” *Antioxid. Basel*, vol. 7, no. 1, 2017, doi: 10.3390/antiox7010004

- [12] Y. Zhang, Z. Qin, W. Sun, F. Chu, and F. Zhou, "Function of Protein S-Palmitoylation in Immunity and Immune-Related Diseases," *Front. Immunol.*, vol. 12, Sep. 2021, doi:10.3389/FIMMU.2021.661202
- [13] M. You et al., "Selenoprotein K contributes to CD36 subcellular trafficking in hepatocytes by accelerating nascent COPII vesicle formation and aggravates hepatic steatosis," *Redox Biol.*, p. 102500, Oct. 2022, doi: 10.1016/j.redox.2022.102500.
- [14] H. Xia et al., "Selenoprotein K Is Essential for the Migration and Phagocytosis of Immature Dendritic Cells," *Antioxidants*, vol. 11, no. 7, p. 1264, Jun. 2022, doi: 10.3390/antiox11071264.
- [15] S.-Z. Jia et al., "Selenoprotein K deficiency-induced apoptosis: A role for calpain and the ERS pathway," *Redox Biol.*, vol. 47, p. 102154, Nov. 2021, doi: 10.1016/j.redox.2021.102154.
- [16] S. Wang, X. Zhao, Q. Liu, Y. Wang, S. Li, and S. Xu, "Selenoprotein K protects skeletal muscle from damage and is required for satellite cells-mediated myogenic differentiation," *Redox Biol.*, vol. 50, p. 102255, Apr. 2022, doi: 10.1016/j.redox.2022.102255
- [17] F. Capone, A. Polo, A. Sorice, A. Budillon, and S. Costantini, "Integrated analysis to study the relationship between tumor-associated selenoproteins: Focus on prostate cancer," *Int. J. Mol. Sci.*, vol. 21, no. 18, p. 6694, 2020.

- [18] M. P. Marciel et al., “Selenoprotein K deficiency inhibits melanoma by reducing calcium flux required for tumor growth and metastasis,” *Oncotarget*, vol. 9, no. 17, pp. 13407–13422, Mar. 2018, doi: 10.18632/oncotarget.24388
- [19] M. P. Marciel and P. R. Hoffmann, “Molecular Mechanisms by Which Selenoprotein K Regulates Immunity and Cancer,” *Biol. Trace Elem. Res.*, vol. 192, no. 1, pp. 60–68, Nov. 2019, doi: 10.1007/S12011-019-01774-8
- [20] M. Bosch et al., “Mammalian lipid droplets are innate immune hubs integrating cell metabolism and host defense,” *Science*, vol. 370, no. 6514, Oct. 2020, doi:10.1126/SCIENCE.AAY8085/SUPPL\_FILE/AAY8085-BOSCH\_REPRODUCIBILITYCHECKLIST.PDF
- [21] E. P. Carpenter, K. Beis, A. D. Cameron, and S. Iwata, “Overcoming the challenges of membrane protein crystallography,” *Current Opinion in Structural Biology*, vol. 18, no. 5, pp. 581–586, Oct. 2008, doi: 10.1016/j.sbi.2008.07.001.
- [22] J. Jumper et al., “Highly accurate protein structure prediction with AlphaFold,” *Nature*, 2021, doi: 10.1038/s41586-021-03819-2.
- [23] P. Tompa, E. Schad, A. Tantos, and L. Kalmar, “Intrinsically disordered proteins: emerging interaction specialists,” *Curr. Opin. Struct. Biol.*, vol. 35, pp. 49–59, Dec. 2015, doi:10.1016/J.SBI.2015.08.009.
- [24] C. O’Shea et al., “Structures and Short Linear Motif of Disordered Transcription Factor Regions Provide Clues to the Interactome of the Cellular Hub Protein

Radical-induced Cell Death1,” *J. Biol. Chem.*, vol. 292, no. 2, p. 512, Jan. 2017, doi: 10.1074/JBC.M116.753426.

[25] M. Kumar et al., “The Eukaryotic Linear Motif resource: 2022 release,” *Nucleic Acids Res.*, vol. 50, no. D1, pp. D497–D508, Jan. 2022, doi: 10.1093/NAR/GKAB975

[26] Z. Huang, F. W. Hoffmann, R. L. Norton, A. C. Hashimoto, and P. R. Hoffmann, “Selenoprotein K is a novel target of m-calpain, and cleavage is regulated by Toll-like receptor-induced calpastatin in macrophages,” *J. Biol. Chem.*, vol. 286, no. 40, pp. 34830–34838, 2011.

[27] J. Song et al., “PROSPER: an integrated feature-based tool for predicting protease substrate cleavage sites,” *PloS One*, vol. 7, no. 11, p. e50300, 2012

[28] D. S. Schwarz and M. D. Blower, “The endoplasmic reticulum: structure, function and response to cellular signaling,” *Cell. Mol. Life Sci.*, vol. 73, no. 1, pp. 79–94, Jan. 2016, doi: 10.1007/s00018-015-2052-6.

[29] T. A. Rapoport, “Protein translocation across the eukaryotic endoplasmic reticulum and bacterial plasma membranes,” *Nature*, vol. 450, no. 7170, pp. 663–669, Nov. 2007, doi: 10.1038/nature06384.

[30] J.-A. Choi and C.-H. Song, “Insights Into the Role of Endoplasmic Reticulum Stress in Infectious Diseases,” *Front. Immunol.*, vol. 10, p. 3147, Jan. 2020, doi: 10.3389/fimmu.2019.03147.

- [31] J. H. Lin, P. Walter, and T. S. B. Yen, “Endoplasmic Reticulum Stress in Disease Pathogenesis,” *Annu. Rev. Pathol. Mech. Dis.*, vol. 3, no. 1, pp. 399–425, Feb. 2008, doi: 10.1146/annurev.pathmechdis.3.121806.151434.
- [32] X. Wu and T. A. Rapoport, “Mechanistic insights into ER-associated protein degradation,” *Current Opinion in Cell Biology*, vol. 53, pp. 22–28, Aug. 2018, doi: 10.1016/j.ceb.2018.04.004.
- [33] Braxton JR, Southworth DR. “Structural insights of the p97/VCP AAA+ ATPase: How adapter interactions coordinate diverse cellular functionality”. *J Biol Chem*. 2023 Nov;299(11):105182. doi: 10.1016/j.jbc.2023.105182.
- [34] Di Xia, Wai Kwan Tang, Yihong Ye. “Structure and function of the AAA+ ATPase p97/Cdc48p”. *Gene*, Volume 583, Issue 1,2016,Pages 64-77, ISSN 0378-1119, <https://doi.org/10.1016/j.gene.2016.02.042>.
- [35] Bing Rao et al.” The cryo-EM structure of an ERAD protein channel formed by tetrameric human Derlin-1”. *Sci. Adv.*7,eabe8591(2021).DOI:10.1126/sciadv.abe8591
- [36] Bing Rao et al. ,The cryo-EM structure of the human ERAD retrotranslocation complex.*Sci. Adv.*9,eadi5656(2023).DOI:10.1126/sciadv.adi5656
- [37] Tomohiro Omura et al. “Endoplasmic Reticulum Stress and Parkinson’s Disease: The Role of HRD1 in Averting Apoptosis in Neurodegenerative Disease” *Oxidative Medicine and Cellular Longevity*, 2013. Volume 2013 | Article ID 239854 | <https://doi.org/10.1155/2013/239854>

- [38] Qi, L., Tsai, B. and Arvan, P. “New insights into the physiological role of endoplasmic reticulum-associated degradation”. *Trends Cell Biol.* 27, 430-440. <https://doi.org/10.1016/j.tcb.2016.12.002>
- [39] F. Ghelichkhani et al., “Selenoprotein S: A versatile disordered protein,” *Archives of Biochemistry and Biophysics*, vol. 731, p. 109427, Nov. 2022, doi: 10.1016/j.abb.2022.109427.
- [40] J. H. Lee et al., “Selenoprotein S-dependent selenoprotein K binding to p97(VCP) protein is essential for endoplasmic reticulum-associated degradation,” *J. Biol. Chem.*, vol. 290, no. 50, pp. 29941–29952, 2015, doi: 10.1074/jbc.M115.680215
- [41] Ye, Y., et al. “Inaugural article: recruitment of the p97 ATPase and ubiquitin ligases to the site of retrotranslocation at the endoplasmic reticulum membrane”. *Proc. Natl. Acad. Sci. U. S. A.* 2005 102:14132–14138

## Chapter 2

### INVESTIGATING THE PHYSIOLOGICAL ROLE OF SELENOPROTEIN K

#### 2.1 Background

Proteins are the molecular workhorses of the cell and they undergo critical post-translational modifications (PTMs) that are pivotal for their structure and function [1]. PTM alter properties of protein by covalent proteolytic cleavage or addition of modifying groups such as acetyl, phosphoryl, glycosyl and methyl, to one or more amino acids [2]. One of the prevalent forms of PTM on proteins is glycosylation [3]. It is estimated that over half of mammalian proteins are glycosylated [4]. There are two major types of protein glycosylation (N-and O-glycosylation), differentiated on the basis of biosynthesis and linkage [5]. O-glycosylation usually occurs after protein folding and export from the ER and it involves the sequential enzymatic addition of glycans to a hydroxyl group of the side chains of amino acids, often serine and threonine[5],[6].

In contrast, N-glycosylation distinguishes itself as a process that takes place during the elongation and folding of proteins in the ER [7]. As nascent proteins traverse the translocon (Sec61 complex) into the ER, the oligosaccharyltransferase (OST) complex catalyze the transfer of a 14 -saccharide core

glucose3-mannose9-acetylglucosamine2) from the dolichol phosphate precursor to a nascent protein at an asparagine (Asn) residue at a recognition site (Asn-X-Ser/Thr) where X is not proline residue on the polypeptide [7],[8], [9]. Next, terminal glucose residues of this core are trimmed by ER glucosidases. Then, with removal of one mannose residue by the ER  $\alpha$ -mannosidase I, the glycoproteins are exported to the Golgi [8], [9].

Some glycoproteins that are trafficked to the plasma membrane move through the Golgi and post-Golgi vesicular compartments to their destination without further processing [8], [9]. These glycans are high-mannose N-glycans. However, the majority undergo additional alterations in the Golgi [9]. Golgi mannosidases remove one to three mannose residues from the core, and various glycosyltransferases (GnTs) then catalyze branching and elongation of the carbohydrate chains, resulting in the formation of hybrid or complex N-glycans [9].

It is also important to note that not all potential N-glycosylation sequons are glycosylated in vivo. It is estimated that about 2/3 of the potential sites are used as substrates by oligosaccharyltransferase [7], [10] and it has been postulated that sequences surrounding the glycosylation site affect glycosylation [7], [11]. In addition, distance from a transmembrane domain in membrane proteins or to the next N-glycosylation site might also influence glycosylation [12].

The diversity of N-glycans across different proteins stems from various factors, including the expression of specific glycosyltransferases in different cell types [13]. Changes in glycosyltransferase expression during cell or tissue development can alter protein

glycosylation patterns [13]. Additionally, amino acid motifs and protein tertiary structure influence glycosylation [14]. Some glycosylation sites are more accessible to Golgi enzymes, leading to the formation of complex N-glycans, while others retain high-mannose or hybrid structures [15], [16]. Consequently, protein glycosylation can vary, with some sites bearing complex N-glycans and others having simpler structures [9].

This modification plays a central role in protein folding, stability, trafficking and quality control in the ER by serving as recognition tags, or sorting signals, that allow glycoproteins to interact with a variety of lectins, glycosidases, and glycosyltransferases ensuring that only properly folded proteins are delivered from the ER to the Golgi [9], [16], [17]. Beyond these functions, N-glycosylation serves as a versatile signaling mechanism, influencing diverse cellular processes. More specifically, it modulates the activity of glycosylated proteins, such as cell surface receptors, and participates in intercellular communication [18], [19], [20].

Proteins also frequently gain functionality through cleavage from their precursor forms. This proteolytic processing, exemplified by proteins like insulin and various growth factors, [21], [22], often results in fragments exerting distinct roles compared to their full-length precursors, participating in signaling cascades or influencing cellular processes [21].

In the context of selenok, we observe both cleaved and glycosylated forms of selenok in vivo. Selenok has an Asn-x-Thr/Ser N-glycosylation recognition site at residues 54, 55, and 56, respectively, with a predicted specific glycosylation at asparagine residue 54 (Asn54)

via an N-acetylglucosamine (GlcNAc) moiety. Studies also suggest that selenok is substrate for calpain proteases, and it is also predicted to be cleaved by serine, cysteine, and metalloproteases [23].

This observation leads to our hypothesis that these modified forms play specific roles in cellular physiology. Drawing parallels with other ER membrane-resident stress regulators, such as activating transcription factor 6 (ATF6) and inositol requiring enzyme 1 IRE1 [24], [25], which undergo activation either by proteolytic cleavage or by cleaving other substrates that aid in alleviating ER stress. We hypothesize that a similar mechanism may occur with selenok. However, the exact regulatory mechanisms governing this process remain unclear.

To explore the physiological role of selenok, we employed cellular fractionation [26] under both stressed and unstressed conditions. The concept of cellular fractionation was pioneered by De Duve and coworkers in 1955 using rat liver tissue [27]. Cellular fractionation is a technique used to isolate different organelles in the cells and has long been used to study protein dynamics in the cell [27], [28]. Subcellular fractionation consists of two major steps: first, the disruption of the cellular organization (homogenization) and secondly, the fractionation of the homogenate to separate the different populations of organelles [28]. This homogenate can then be separated by differential centrifugation into several fractions such as nucleus, mitochondria, cytosol, and lysosomes. Each population of organelles is characterized by size, density, charge and other properties on which the

separation relies. This cellular fractionation approach aims to elucidate the cellular localization patterns of selenok, providing insights into its dynamic behavior during stress.

Although cellular fractionation is a prevalent method for studying the localization and function of nuclear proteins, it faces challenges [29]. These challenges involve selectively permeabilizing the plasma membrane while safeguarding the nuclear membrane's integrity to ensure the nucleus remains undisturbed. Secondly, the temperature sensitivity of facilitated nuclear transport pathways poses a risk of mis-localizing nuclear proteins during prolonged, low-temperature incubations in fractionation procedures. The third challenge involves the leakage of small proteins through nuclear pore complexes (NPCs). Even with a fully intact nuclear envelope (NE), proteins smaller than approximately 60 kDa may seep out through these complexes [29].

Furthermore, to confirm the presence of N-glycosylation in selenok, we conducted a Peptide-N-Glycosidase F (PNGase F) assay. PNGase F is a glycosidase enzyme derived from the bacterium *Flavobacterium meningosepticum* [30], efficient in removing N-linked glycans from glycoproteins for subsequent analysis [31]. By cleaving these glycans from asparagine residues, we can confirm the nature of the glycosylation on selenok. Our investigation aims to chart selenok's post-translational modifications and their impact on cellular stress responses

## **2.2 Results**

### **2.2.1 Cellular localization of selenoprotein k in fractionated mammalian cells**

The earliest subcellular fractionation method involves physically disrupting cells or tissues, followed by sequential centrifugation to isolate organelles like nuclei, mitochondria, and lysosomes [32]. However, this method has limitations, often resulting in mixed fractions with organelles of similar sedimentation velocities [28]. Newer techniques address these challenges by using non-physical methods such as detergents or hypo-osmotic shock to replace the initial homogenization step [26], [29], [33], [34]. For example, NP-40, a detergent, is commonly used, sometimes skipping density-based isolation steps. Another approach is using digitonin to selectively permeabilize the plasma membrane (PM), preserving nucleus integrity [29], [34], [35]. Recent advancements in subcellular fractionation focus on enhancing accuracy and specificity. These include using low concentrations of mild detergents like digitonin to maintain nucleus integrity, employing lectins to prevent protein loss from the nucleus, and varying cell conditions with different buffers during permeabilization and density-dependent cell separation [29][35].

To overcome challenges in cellular fractionation, we adopted a method refined by Ogawa et al 2021. This method entailed optimizing conditions, such as treatment temperature, to selectively permeabilize plasma membranes using a specified concentration of digitonin, along with treating cells with the lectin wheat germ agglutinin (WGA), which prevents leakage of small proteins from the nucleus. However, in our study, we deliberately omitted

WGA to mitigate potential concentration effects on glycosylated proteins, thereby minimizing the risk of obtaining inaccurate results.

This method divides the cell into cytosolic (C) and nuclear fractions. The nuclear fraction is further subdivided into the nuclear soluble (NS) fraction, which contains soluble nuclear proteins, and the nuclear pellet (NP) fraction, which comprises the nuclear membrane and other insoluble nuclear proteins. However, separating the ER, where selenok is located, from the nucleus poses a challenge. As a result, the NP may contain both ER membrane proteins and insoluble nuclear proteins.

In our experimental setup, stable cell lines expressing HA-TEV-selenok U92C (MW -12.8 kDa) were utilized. From a total of 10 million cultured cells, 5 million underwent ER stress induction with 1 µg/ml tunicamycin [36], while the remaining 5 million were grown without inducing ER stress. For each condition (stress and unstressed), 0.5 million cells were collected as whole cells, and the remaining 4.5 million cells were subjected to fractionation with 100 µg/mL digitonin. Different centrifugation speeds were employed following the protocol to isolate subcellular fractions.

Anti-selenok western blot analysis of fractionated cells revealed the presence of HA TEV selenok 1-94 in both cytosolic and nuclear fractions. Approximately 10% of selenok was observed in the cytosolic fraction (C), whereas in the nuclear fractions, 90% was found in the nuclear pellet (NP), with none in the nuclear soluble fraction (NS) as depicted in Figure 2.1. A significant observation was the increase in the expression of the shorter form of

selenok (HA TEV selenok 1-79) during ER stress induced by tunicamycin, shown in Figure 2.1. These findings further suggest that selenok might undergo cleavage during ER stress and strengthen our hypothesis that these truncated forms may migrate to the nucleus, potentially acting as regulatory factors or cofactors for genes involved in alleviating ER stress. These findings serve as a foundation for a more in-depth exploration of selenok's role in cellular stress responses

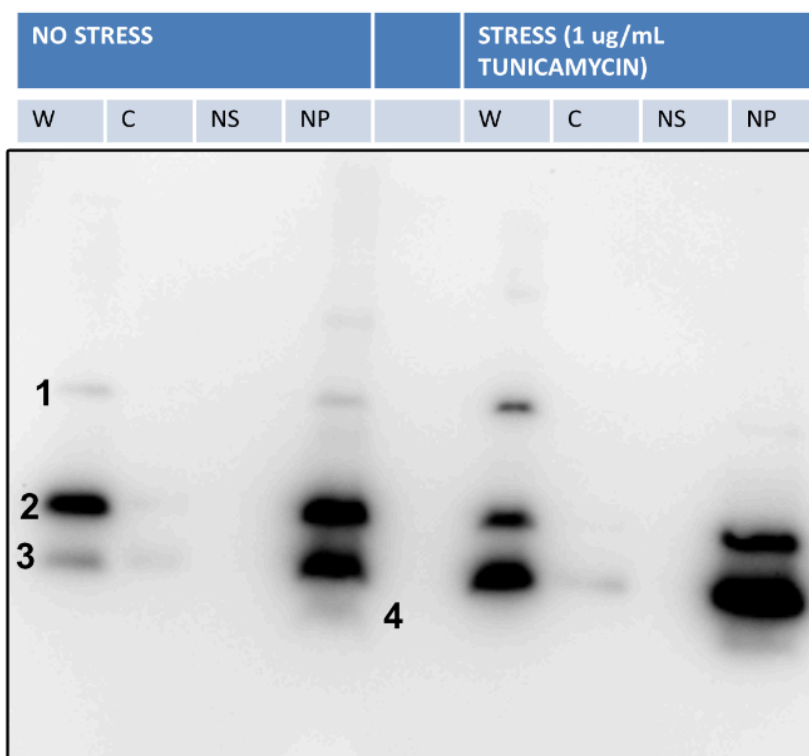


**Figure 2.1: Anti-selenok western blot of overexpressed HA TEV selenok 1-94 in fractionated HEK 293 cells during stress and unstressed conditions.** ER stress was induced in 5 million cells using 1  $\mu$ g/ml tunicamycin, while another 5 million cells were left untreated. Whole-cell lysates (W) were obtained from 0.5 million cells, and the remaining 4.5 million cells in each condition were fractionated into cytosolic (C), nuclear soluble (NS), and nuclear pellet (NP) fractions. Overexpressed HA TEV selenok 1-94 U92C, 12.8 kDa (1) is evident in W, C, and NP fractions. Importantly, two cleaved forms of this construct, HA TEV selenok 1-79, 11.5 kDa (2) and HA TEV selenok 1-71, 10.5 kDa (3) are also observed, with (2) increasing during ER stress. In addition, an oligomerized form of this construct was also observed (4). (n=1)

### **2.2.2 Identification of N-Glycosylation in Selenoprotein k**

As previously mentioned, selenok possesses an Asn-x-Thr/Ser N-glycosylation recognition site at residues 54, 55, and 56, respectively, with a predicted specific glycosylation at asparagine residue 54 (Asn54) via an N-acetylglucosamine (GlcNAc) moiety. We have previously shown that mutation of Asn 54 resulted in removal of glycosylated forms of selenok [37]. PNGase F is a glycosidase enzyme derived from the bacterium *Flavobacterium meningosepticum* [30], efficient in hydrolyzing N-linked glycans from glycoproteins for subsequent analysis [31]. By enzymatically hydrolyzing N-glycan from selenok with PNGase F, this study provides support for N-glycosylation in selenok.

In this study, two million Flp-in HEK 293 cells were transfected with V5 selenok U92C 1-94 and cultured in DMEM media supplemented with 10% FBS and 1% Penstrep. Following cell harvest, lysed cells were divided into three groups, each containing an equal amount of protein. These groups were treated with 0 mg/ml (1 ul water), 0.05 mg/ml (1  $\mu$ l), and 0.5 mg/ml (1  $\mu$ l) of purified PNGase F respectively. Cell samples were collected at 0, 20, and 60 minutes of incubation with the enzyme at 37°C.

Anti-V5 western blot revealed the hydrolysis of N-glycosylated selenok in all concentrations of PNGase F at all incubation times (0, 20, and 60 mins), except for those treated with no PNGase F (1  $\mu$ l water), as depicted in Figure 2.2. Additionally, other cleaved and oligomerized selenok forms were observed.

This study provides further support that selenok is indeed N-glycosylated, supporting and reinforcing our hypothesis that these various glycosylated forms might play crucial physiological roles in mitigating ER stress.

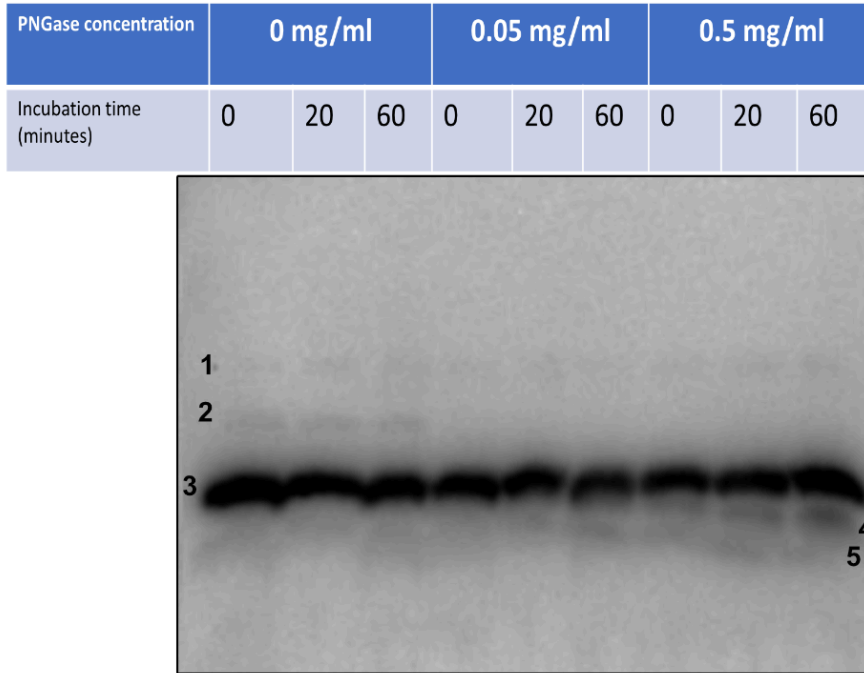


**Figure 2.2: Anti-V5 westerns of overexpressed V5 selenok U92C 1-94 at different PNGase F concentrations and incubation times at 37°C in Flp-in HEK 293 cells.** Overexpressed V5-tagged selenok U92C 1-94, 12 kDa (3) was detected in all samples. Glycosylated forms of V5-tagged selenok U92C 1-94 (2) were only observed in samples treated with no PNGase. Additionally, two cleaved forms corresponding to V5-tagged selenok 1-79 (4, 10.5 kDa) and V5-tagged selenok 1-71 (5, 9.5 kDa) were detected, along with an oligomerized form of V5-tagged selenok 1-94 U92C. (n=1)

### **2.3 Discussion**

In vivo Investigation of selenok forms and cellular localization during ER stress conditions forms an essential step in understanding its physiological role. Our result shows the presence of cleaved selenok and N-glycosylated forms of selenok in vivo. Notably, the level of the shorter variant selenok (1-79) increased during stress, which suggests a potential role in addressing ER stress.

Interestingly, selenok was not observed in the nuclear soluble fraction, raising the possibility of leakage during fractionation. Proteins smaller than 60 kDa are prone to leaking from the nucleus during this process [29]. In addition, distinguishing the nucleus from the ER membrane poses a challenge [19], and what we term the "nuclear pellet" may encompass both ER membrane proteins and nuclear insoluble components.

The complexity of the ER and nuclear membrane interface poses a formidable challenge, and refining our fractionation techniques could provide more accurate insights into selenok's subcellular distribution. In addition to fractionation, employing immunofluorescence microscopy with antibodies targeting different fragments of selenok emerges as a valuable strategy. This technique offers a more direct visualization of selenok's location during ER stress, complementing our fractionation data.

## 2.4 Methods

### 2.4.1 Cell culture and expression of selenok constructs

Expression vector ID	Construct
SR_110_21	HA-TEV-selenok U92C 1-94
SR_10_150	V5 selenok U92C 1-94

**Table 2.1: The vector numbers and their corresponding selenok construct**

Stable HEK 293 cell lines expressing HA-TEV-selenok U92C (SR\_110\_21) were used for this study. Two million cells were seeded in a T75 flask (at confluence we had ~ ten million cells). Among these, 5 million cells were cultured without inducing stress, while an additional 5 million HEK 293 cells were subjected to ER stress induction by adding 1 µg/ml tunicamycin four hours before initiating expression with 50 ng/ml tetracycline. The cell growth and maintenance occurred in DMEM supplemented with 10% FBS and 1% Penstrep.

For the expression of V5-selenok U92C 1-94, around 0.7 million Flp-in HEK 293 cells were seeded into a T25 flask. Plasmid DNA was diluted in serum-free DMEM media, with 2.5 µL of DNA plasmid added to 100 µL of serum-free DMEM. The PolyJET reagent was diluted by combining 7.5 µL of PolyJET reagent with 100 µL of serum-free DMEM. The diluted DNA and PolyJET reagent were mixed to form DNA-PolyJET complexes. Following the removal of old media from the wells of a 6-well plate, 2800 µL of fresh media was added to each well. Subsequently, 200 µL of the DNA-PolyJET mixture was dropwise added to each well, ensuring uniform distribution of the complexes. The cells

were then incubated at 37°C for 48 hours to facilitate transfection, allowing the cells to recover and express the transfected plasmid construct. The cells were further incubated for an additional 48 hours to promote adherence and reach approximately 60% confluence.

#### **2.4.2 Cellular fractionation**

Whole cell lysate from 0.5 million cells in two tubes was collected initially. The remaining 4.5 million cells underwent fractionation. Cells were centrifuged at 2,000 g for 30 sec, and the supernatant was aspirated. Cell pellets were gently mixed with 400 µL of pre-warmed TB (Transfer Buffer) and centrifuged. After aspirating the supernatant, pellets were mixed with 400 µL of 100 µg/mL digitonin. Supernatants were collected after centrifugation. This process was repeated, and the resulting supernatants constituted the cytosolic fraction (800 µL).

For nuclear fractions, cell pellets were successively treated with ice-cold TB, and after centrifugation, the supernatants were collected. The remaining pellets were resuspended in ice-cold PBS (-) with inhibitors, frozen-thawed, and centrifuged at 21,500 g for 10 minutes at 4°C. Supernatants and final insoluble fractions were designated as nuclear soluble and pellet fractions, respectively, using an Optima max XP ultracentrifuge. Pellets were sonicated and resolved in a 1x sample buffer. All fractions, except the pellet fractions, were acetone-precipitated using four times the volume of pre-chilled acetone at -30°C for 4 hours.

### **2.4.3 Acetone precipitation**

Following the protocol, acetone precipitation was applied only to the cytosolic and nuclear soluble fractions. Acetone was cooled to  $-20^{\circ}\text{C}$ , and an acetone-compatible tube was used for protein samples. Cold acetone, four times the sample volume, was added to the sample in the tube, vortexed, and incubated for 4 hours at  $-20^{\circ}\text{C}$ . Centrifugation at 13,000-15,000  $\times$  g for 10 minutes followed, and the supernatant was carefully decanted to avoid disturbing the protein pellet. If needed, additional precipitation cycles were performed before allowing the acetone to evaporate for 5 minutes at room temperature in an uncapped tube. Over-drying was avoided, and the pellet was dissolved in lysis buffer by thorough vortexing for downstream processing.

### **2.4.4 Harvest and lysis**

The cells were removed from well by trypsin and incubated at  $37^{\circ}\text{C}$  for approximately 3 minutes. Neutralization was achieved by adding media to each well. After transferring the cell suspension to a collection tube and centrifuging at 300 g for 5 minutes at  $4^{\circ}\text{C}$ , the media was carefully decanted, and cells were resuspended in PBS. Another centrifugation at 300 g for 5 minutes at  $4^{\circ}\text{C}$  followed, and the PBS was decanted. Lysis of cells involved the addition of 200  $\mu\text{L}$  ice-cold lysis buffer (25 mM Tris-HCl pH 7.4, 150 mM NaCl, 1% IGEPAL CA-630, 1 mM EDTA, 5% glycerol), supplemented with Halt Protease Inhibitor and phosphatase inhibitors just before use. After a 20-minute incubation on ice for protein extraction, the lysed cells were spun down at 12,000 g for 20 minutes at  $4^{\circ}\text{C}$ . The collected supernatant (lysate) was carefully transferred to new tubes without disturbing the pellet.

#### **2.4.5 Measuring protein concentration**

Protein concentrations of the lysate were analyzed using the Bradford assay. 1  $\mu$ L of the lysate were added into 1000  $\mu$ L of Bradford reagent and mixed thoroughly. Absorbance was measured at 595 nm and the protein concentrations calculated.

#### **2.4.6 PNGase concentration and assay**

We employed a 3 kDa molecular weight cut-off (MWCO) Amicon concentrator for PNGase (~36 kDa), ensuring efficient retention of most proteins. Loading the concentrator with 1 ml of the initial PNGase, which had a concentration of 0.1 mg/ml, achieved a final concentration of approximately 1 mg/ml. The centrifugation at 4,000 rpm for 20 minutes was repeated until the final volume reached 100  $\mu$ l. Following centrifugation, the concentrated protein solution was carefully withdrawn from the concentrator.

The cell lysate was divided into three segments, each containing 50  $\mu$ l of lysate. One segment received 1  $\mu$ l of distilled water, while the other two segments received 1  $\mu$ l of 0.05 mg/ml and 0.5 mg/ml PNGase F, resulting in a total reaction volume of 51  $\mu$ l. The mixture underwent incubation at 37°C, and 16  $\mu$ l of cell lysate were sampled at 0, 20, and 60 minutes, respectively.

#### **2.4.7 Tricine SDS-PAGE gel**

To conduct Tricine SDS-PAGE [38] analysis, we utilized a gel system comprising a 16% separating gel with glycerol and a 4% stacking gel. The 16% separating gel was prepared using Fisher BioReagents Acrylamide:Bis-Acrylamide 19:1 (40% Solution, 5% cross-linking), while the 4% stacking gel was prepared with Apex Acrylamide:Bis-Acrylamide 37.5:1 (40% solution, 2.6% cross-linking). Samples were prepared with 4X sample buffer, subsequently diluted to 1X with sample buffer, and loaded onto the tricine gel under reducing conditions. Gel electrophoresis was conducted at 90 V for 20 minutes, followed by an increase to 140 V for an additional 60 minutes. The gels were then prepared for transfer onto a PVDF membrane for subsequent western blot analysis.

#### **2.4.8 Western blotting**

The PVDF (polyvinylidene fluoride) membrane underwent activation through a brief soak in methanol. Filter paper, saturated with a transfer buffer, was prepared. The assembly involved layering filter paper, membrane, gel, and another filter paper. Semi-dry transfer occurred using a Biorad semi-dry trans-turbo system for 15 minutes at 20 V and 1 A. Post-transfer, the membrane underwent blocking in a buffer with 5% BSA in TBST for 30 minutes. Primary antibodies specific to the V5 tag (Thermo anti-V5 antibody, Catalog # R96025) and selenok (Invitrogen anti-selenok, Cat # PA5-34420) were applied at a 1:2000 dilution in TBST and incubated for 1 hour. The membrane was washed thrice with TBST for 5 minutes each to eliminate unbound primary antibodies. Secondary antibodies

(anti-mouse and anti-rabbit, both from Proteintech) were applied at a 1:20000 dilution in TBST and incubated for 1 hour. After three washes with TBST for 5 minutes each, chemiluminescence substrate and enhancer were applied to the membrane. A mixture of 1.4 ml (750  $\mu$ L each) was evenly spread across the membrane. Upon activation of the chemiluminescent signal detection system, the membrane image was captured using a ChemFlour R imager. Western blot results were analyzed, and band intensities were quantified.

## REFERENCES

- [1] Conibear, Anne C. "Deciphering protein post-translational modifications using chemical biology tools." *Nature Reviews Chemistry* 4.12 (2020): 674-695.
- [2] Shahin Ramazi, Javad Zahiri, "Post-translational modifications in proteins: resources, tools and prediction methods," *Database*, Volume 2021, 2021, baab012, <https://doi.org/10.1093/database/baab012>
- [3] Schjoldager, Katrine T., et al. "Global view of human protein glycosylation pathways and functions." *Nature reviews Molecular cell biology* 21.12 (2020): 729-749.
- [4] Krištić, Jasminka, and Gordan Lauc. "Ubiquitous importance of protein glycosylation." *High-Throughput Glycomics and Glycoproteomics: Methods and Protocols* (2017): 1-12.
- [5] Zauner, Gerhild, et al. "Protein O-glycosylation analysis." *Biological chemistry* 393.8 (2012): 687-708.
- [6] Reily, Colin, et al. "Glycosylation in health and disease." *Nature Reviews Nephrology* 15.6 (2019): 346-366.
- [7] Hevér, Helga, et al. "Characterization of site-specific N-glycosylation." *Post-Translational Modification of Proteins: Tools for Functional Proteomics* (2019): 93-125.

- [8] Cherepanova, Natalia, Shiteshu Shrimal, and Reid Gilmore. "N-linked glycosylation and homeostasis of the endoplasmic reticulum." *Current opinion in cell biology* 41 (2016): 57-65.
- [9] Vagin, Olga, Jeffrey A. Kraut, and George Sachs. "Role of N-glycosylation in trafficking of apical membrane proteins in epithelia." *American Journal of Physiology-Renal Physiology* 296.3 (2009): F459-F469.
- [10] D.F. Zielinska, et al. "Precision mapping of an in vivo N-glycoproteome reveals rigid topological and sequence constraints". *Cell* 141 (2010) 897–907
- [11] Huang, Yen-Wen, et al. "Residues comprising the enhanced aromatic sequon influence protein N-glycosylation efficiency." *Journal of the American Chemical Society* 139.37 (2017): 12947-12955.
- [12] I.M. Nilsson, et al. "Determination of the distance between the oligosaccharyltransferase active site and the endoplasmic reticulum membrane". *J. Biol. Chem.* 268 (1993) 5798–5801
- [13] Toustou, Charlotte, et al. "Towards understanding the extensive diversity of protein N-glycan structures in eukaryotes." *Biological Reviews* 97.2 (2022): 732-748.
- [14] Huang, Yen-Wen, et al. "Residues comprising the enhanced aromatic sequon influence protein N-glycosylation efficiency." *Journal of the American Chemical Society* 139.37 (2017): 12947-12955.
- [15] Cherepanova, Natalia, Shiteshu Shrimal, and Reid Gilmore. "N-linked glycosylation and homeostasis of the endoplasmic reticulum." *Current opinion in cell biology* 41 (2016): 57-65.

- [16] Hebert, Daniel N, and Maurizio Molinari. "In and out of the ER: protein folding, quality control, degradation, and related human diseases." *Physiological reviews* 87.4 (2007): 1377-1408.
- [17] Cherepanova, Natalia, et al. "N-linked glycosylation and homeostasis of the endoplasmic reticulum." *Current opinion in cell biology* 41 (2016): 57-65.
- [18] Yoshimi Haga, et al. "N-Glycosylation Is Critical for the Stability and Intracellular Trafficking of Glucose Transporter GLUT4". *Journal of Biological Chemistry*, Volume 286, Issue 36, 2011, Pages 31320-31327, ISSN 0021-9258, <https://doi.org/10.1074/jbc.M111.253955>.
- [19] Gregorczyk, P, et al. "N-glycosylation acts as a switch for FGFR1 trafficking between the plasma membrane and nuclear envelope". *Cell Commun Signal* 21, 177 (2023). <https://doi.org/10.1186/s12964-023-01203-3>
- [20] Hang, Qinglei, et al. "Integrin  $\alpha 5$  suppresses the phosphorylation of epidermal growth factor receptor and its cellular signaling of cell proliferation via N-glycosylation." *Journal of Biological Chemistry* 290.49 (2015): 29345-29360.
- [21] Lichtenthaler, Stefan F., Marius K. Lemberg, and Regina Fluhrer. "Proteolytic ectodomain shedding of membrane proteins in mammals—hardware, concepts, and recent developments." *The EMBO journal* 37.15 (2018): e99456.
- [22] Docherty K et al, "Conversion of proinsulin to insulin: involvement of a 31,500 molecular weight thiol protease." *PNAS* August 1, 1982, 79 (15) 4613 4617 <https://www.pnas.org/doi/abs/10.1073/pnas.79.15.4613>

- [23] J. Song et al., "PROSPER: an integrated feature-based tool for predicting protease substrate cleavage sites," *PloS One*, vol. 7, no. 11, p. e50300, 2012.
- [24] Jingshi Shen, Ron Prywes, "ER stress signaling by regulated proteolysis of ATF6", *Methods*, Volume 35, Issue 4, 2005, Pages 382-389, ISSN 1046-2023, <https://doi.org/10.1016/j.ymeth.2004.10.011>.
- [25] Chalmers F et al. "Inhibition of IRE1 $\alpha$ -mediated XBP1 mRNA cleavage by XBP1 reveals a novel regulatory process during the unfolded protein response". *Wellcome Open Res.* (2017) Oct 9;2:36. doi: 10.12688/wellcomeopenres.11764.2. PMID: 29062910; PMCID: PMC5645705.
- [26] Suzuki, K., et al. "REAP: A two-minute cell fractionation method". *BMC Res Notes* 3, 294 (2010). <https://doi.org/10.1186/1756-0500-3-294>
- [27] De Duve, Christian, et al. "Tissue fractionation studies. 6. Intracellular distribution patterns of enzymes in rat-liver tissue." *Biochemical Journal* 60.4 (1955): 604.
- [28] Lee, Yie Hou, Hwee Tong Tan, and Maxey CM Chung. "Subcellular fractionation methods and strategies for proteomics." *Proteomics* 10.22 (2010): 3935-3956.
- [29] Ogawa, Y., & Ogawa, N. "Methods to separate nuclear soluble fractions reflecting localizations in living cells". *iScience*. 2021, 24(12). <https://doi.org/10.1016/j.isci.2021.103503>
- [30] Ling Hua, et al. "Highly efficient production of peptides: N-glycosidase F for N-glycomics analysis, *Protein Expression and Purification*", Volume 97, 2014, Pages 17-22, ISSN 1046-5928, <https://doi.org/10.1016/j.pep.2014.02.004>.

- [31] Szigeti, M. et al. "Rapid N -glycan release from glycoproteins using immobilized PNGase F microcolumns" *Journal of chromatography*, 2016, Vol.1032,
- [32] Jung, Eva, et al. "The establishment of a human liver nuclei two-dimensional electrophoresis reference map." *ELECTROPHORESIS: An International Journal* 21.16 (2000): 3483-3487.
- [33] Liu, Xiaoyong, and François Fagotto. "A method to separate nuclear, cytosolic, and membrane-associated signaling molecules in cultured cells." *Science signaling* 4.203 (2011): pl2-pl2.
- [34] Kimura, Makoto, et al. "Novel approaches for the identification of nuclear transport receptor substrates." *Methods in Cell Biology*. Vol. 122. Academic Press, 2014. 353-378.
- [35] Thakar, Ketan, et al. "Identification of CRM1-dependent nuclear export cargos using quantitative mass spectrometry." *Molecular & Cellular Proteomics* 12.3 (2013): 664-678.
- [36] Xiaoyong L, François F. "A Method to Separate Nuclear, Cytosolic, and Membrane-Associated Signaling Molecules in Cultured Cells." *Sci. Signal.* 4,pl2-pl2(2011).DOI:10.1126/scisignal.2002373
- [37] Cheng, Rujin. *The Function of Intrinsically Disordered Selenoproteins*, University of Delaware, United States -- Delaware, 2020. ProQuest, <https://www.proquest.com/dissertations-theses/function-intrinsically-disordered-selenoproteins/docview/2781613263/se-2>.
- [38] H. Schägger, "Tricine-SDS-PAGE," *Nat Protoc*, vol. 1, no. 1, pp. 16-22, Jun. 2006, doi: 10.1038/nprot.2006.4.

## Chapter 3

### PURIFICATION OF SELENOPROTEIN K AND ITS ERAD PARTNERS P97

#### ATPASE AND SELENOPROTEIN S

##### 3.1 Background

ERAD is the cellular machinery responsible for the retro-translocation of misfolded proteins from the ER for proteasomal degradation in the cytosol [1]. Dysregulation of ERAD has been implicated in various diseases and cancers [2], [3]. In ERAD, derlins, p97 ATPase, and ubiquitin ligases have shown to be crucial for misfolded protein retro-translocation [4],[5],[6]. Selenok has shown to interact with key players of ERAD including derlins, p97 ATPase, and selenos [7]. In the ER, derlins couple with ER-resident ubiquitin ligases in defining convergent ERAD pathways, and studies have shown selenok and selenos to have different affinities for derlins [7]. This poses the question of whether selenok or selenos is connected to certain ubiquitin ligases and corresponding ERAD pathways through association with derlins. p97 ATPase, on the other hand, is directly recruited by selenos to the ER membrane via a VCP interacting motif (VIM) within residues 69-108 [8]. Recent studies suggest that selenok interacts indirectly with p97 through its association with selenos [9]. However, neither the mechanistic details of these interactions at an atomic level nor the role of selenok in ERAD are fully understood

One of the methods for studying protein interaction and complexes at an atomic level is via structural characterization by x-ray crystallography. However, this method faces challenges due to the hydrophobic nature of membrane proteins as well as the presence of IDR in some membrane proteins, making traditional crystallization methods difficult [10]. Unlike crystallographic approaches, single-particle cryo-electron microscopy (cryoEM) determines structures of biological macromolecules by averaging electron microscopy images of target molecules embedded in a thin layer of vitreous ice in random orientations [11], [12]. Because it does not require either crystallization or absolute sample homogeneity, it has been used to study large membrane complexes that are obviously refractory to crystallization [11], [13].

The structure of selenok has not been characterized however, a structural model of selenok is available based on AlphaFold2 [14]. According to this prediction, selenok spans 94 residues, exhibiting three distinct segments: residues 1-19 constitute the short N-terminus, residues 20-51 form a membrane-bound hydrophobic helix, and residues 51-94 comprise the intrinsically disordered C-terminus. The disordered C-terminus is rich in polar residues, prominently featuring proline, and contains Sec at position 92. (figure 3.1 B). Selenok also possesses interaction hubs for interacting with its protein partners. ELM predicts the presence of two SH2 binding elements in selenok: one located at the N-terminus (residues 3-6) and another in the disordered C-terminus (residues 60-63). Additionally, three SH3 binding sites are predicted within the disordered region: residues 64-70 for class I SH3

domains, residues 67-70 for class II SH3 domains, and a third site at residues 80-86 (figure 3.1 A).

Structural characterization by cryo-EM requires the extraction and purification of selenok and its ERAD partners. By purifying selenok's membrane and IDR segment as well as its ERAD partners p97 and selenos, this work aims to provide a foundation for further investigative structural studies by cryo-EM. The goal is to elucidate the interaction between selenok and its partners selenos and p97, ultimately shedding light on its role in the ERAD.

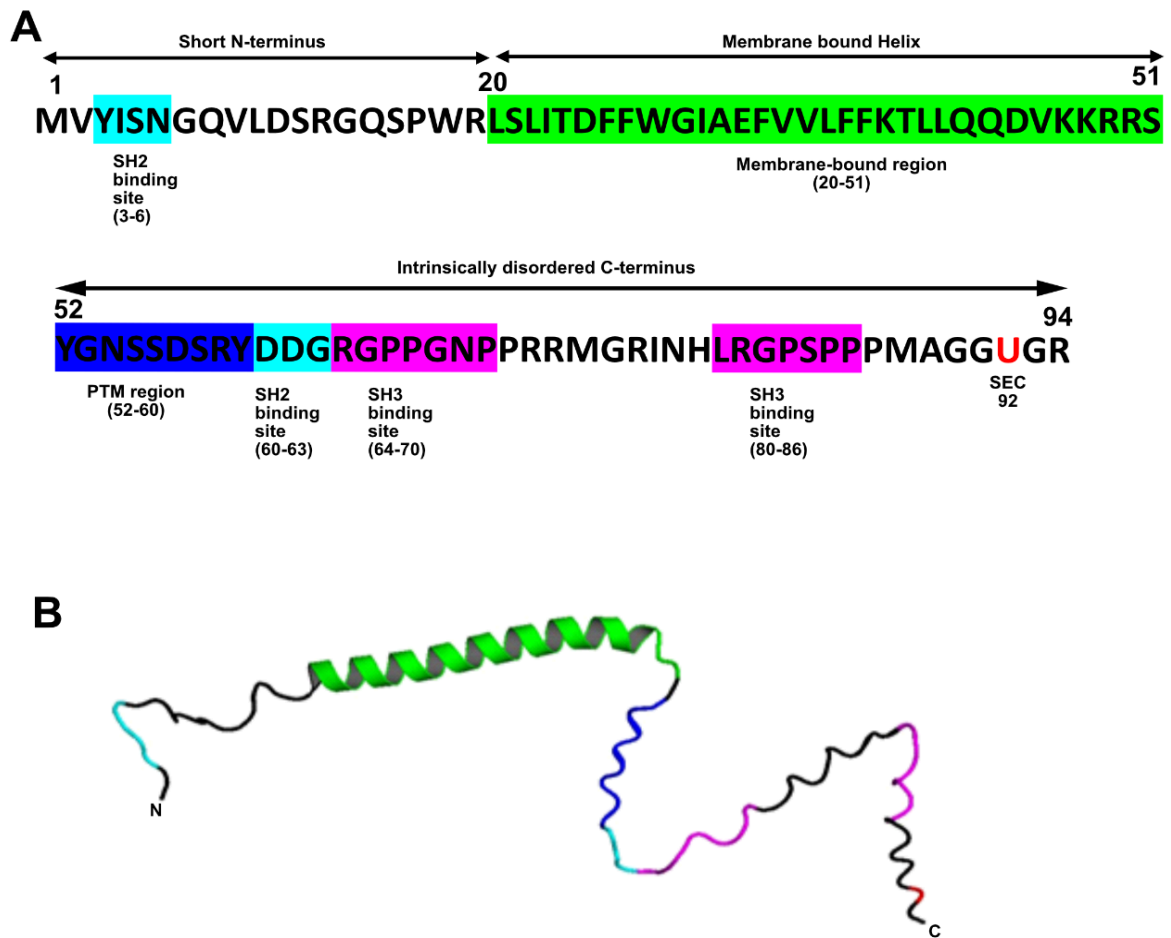


**Figure 3.1: AlphaFold2 prediction of Human selenok.** (A) AlphaFold2 segmentation of human selenok. Also included are ELM predicted motifs. (B) AlphaFold2 structural prediction of human selenok.

### **3.3 Results**

#### **3.2.1 Purification of selenoprotein k (2-42 & 43-94)**

According to the AlphaFold2 prediction [14], selenok's membrane-interacting region spans residues 20 to 51, while the disordered region extends from residue 52 to 94 on the C terminus (see Figure 1.2). To facilitate future investigative studies, we purified both the membrane portion (residues 2-42) containing the short N-terminus (residue 1-20) and the disordered region (residues 43-94) of selenok. It's noteworthy that we had previously purified the full-length selenok (1-94) as reported [15].

Selenok was expressed as a fusion protein with Maltose Binding Protein (MBP) in *E. coli* to enhance stability and solubility [15]. While MBP-selenok remains soluble and localized in the cytosol during expression, it can aggregate post-purification in the absence of detergents [15]. Therefore, for purifying the membrane portion of selenok, it was imperative to conduct the extraction in the presence of DDM, Triton X-100 or other suitable detergents to prevent aggregation. Selenok 2-42 (6x His-tagged MBP TEV strep selenok 2-42) was expressed as a MBP fusion in *E. coli*, and the fusion protein was subsequently purified via immobilized metal affinity chromatography (IMAC). Following cleavage from its MBP partner by TEV protease, the strep-tagged selenok 2-42 was isolated from the 6x His-tagged TEV protease and MBP using Strep-Tactin XL 4Flow resin. The final purified protein exhibited a purity exceeding 95% (see Figure 3A & B).

Similarly, selenok 43-94 was expressed as a MBP fusion protein (6x His-tagged MBP TEV strep selenok 43-94 U92C) in *E. coli*, but it was extracted without detergents, as the absence of the membrane-interacting region eliminated the risk of aggregation. Following TEV cleavage, strep-tagged selenok 43-94 U92C was subjected to desalting and further purification using cation exchange chromatography. The resulting purified protein exhibited a purity exceeding 90% and included other oligomerized forms of the protein (see Figure 3.2 C & D).

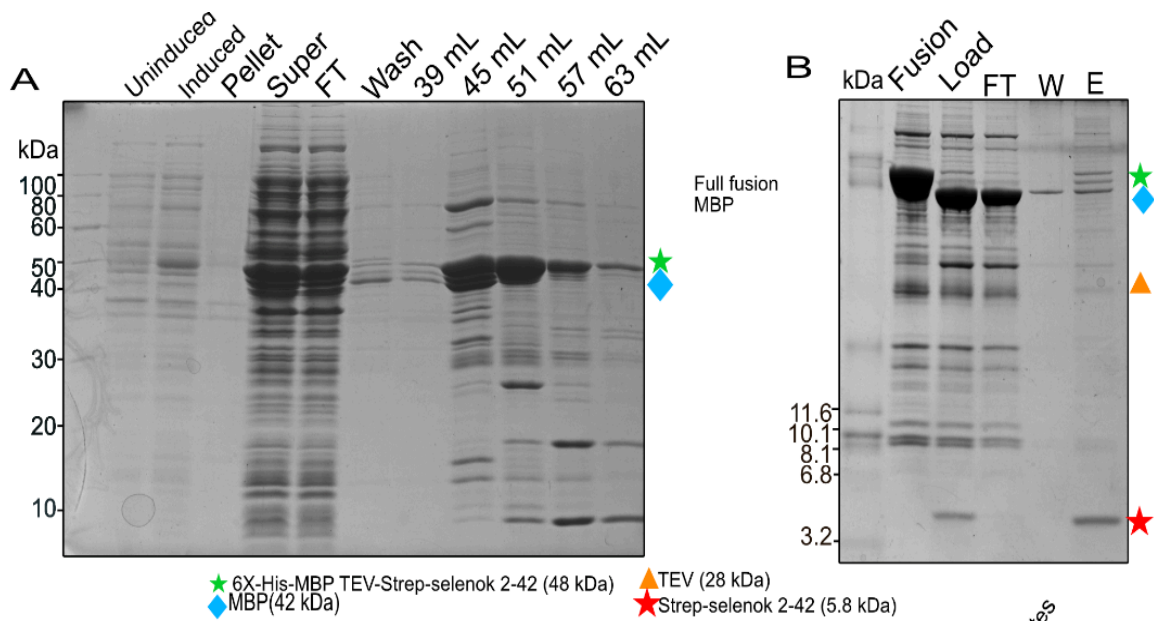


**Figure 3.2: IMAC and Strep-Tactin purification of selenok 2-42.** 16% glycine (A) and 16 % tricine (B) SDS-PAGE (reducing condition) analysis of selenok 2-42 purification. (A) 6x His-MBP-TEV-selenok 2-42 was purified using an IMAC to separate the His-tagged fusion protein from cell lysates. (B) IMAC eluates were incubated with TEV protease and subsequently purified using a Strep-Tactin XL 4Flow resin to isolate the strep-tagged selenok 2-42 from the TEV protease and MBP. (SDS-PAGE analysis was carried out by George Woodward)

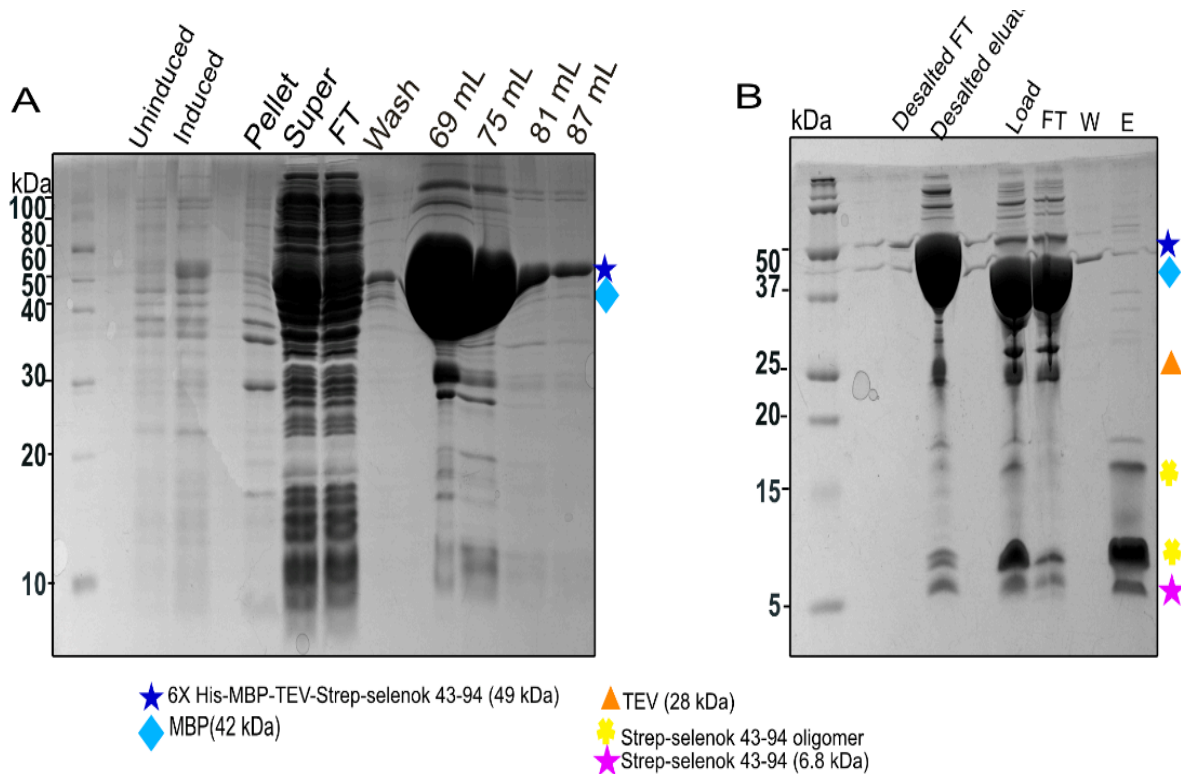


**Figure 3.3: IMAC and cation IEX (SP) chromatography purification of selenok 43-94 U92C.** 16% glycine (A) and 16 % tricine (B) SDS-PAGE (reducing condition) analysis of selenok 43-94 U92C purification. (A) 6x His-MBP-TEV-selenok 43-94 U92C was purified using an IMAC to separate the His-tagged fusion protein from cell lysates (B) IMAC eluates were desalted, incubated with TEV protease, and subsequently purified using cation IEX (SP) chromatography to isolate the strep-tagged selenok 43-94 U92C from the TEV protease and MBP.

### 3.2.2 Purification of p97 ATPase

One of the ERAD partners that selenok has shown to interact with is the hexameric ATPase p97 [6], [7]. We purified p97 by IMAC and size exclusion chromatography (SEC). A p97 vector with a C-terminal His tag (p97 His) was expressed in *E. coli* Rosetta cells. Subsequently, the p97 His was purified via IMAC using a Ni<sup>2+</sup>-charged IMAC column to separate it from the cell lysates (Figure 3.3 A). The eluted p97 His fractions from IMAC were further concentrated and subjected to size exclusion chromatography using a Sephacryl S-300 HR column.

As shown in Figure 3.3 B, p97 was observed to elute from the SEC column between 35 mL to 50 mL of elution volume. The elution profile indicated that the p97 dodecamer exhibited an earlier peak elution volume compared to the p97 hexamer. Specifically, the p97 dodecamer peaked at 40 mL, whereas the p97 hexamer fragment showed a peak elution at 45 mL (Figure 3.3 B). Based on the calibration curve of the Sephacryl S-300 HR column established with globular proteins, we estimated the molecular weights of the eluted p97 hexamer and dodecamer to be approximately 1000 kDa and 552 kDa, respectively.

Furthermore, these fractions were subsequently analyzed on a glycine SDS-PAGE gel to confirm their purity (Figure 3.3 C). The p97 exhibited a purity level exceeding 95%.

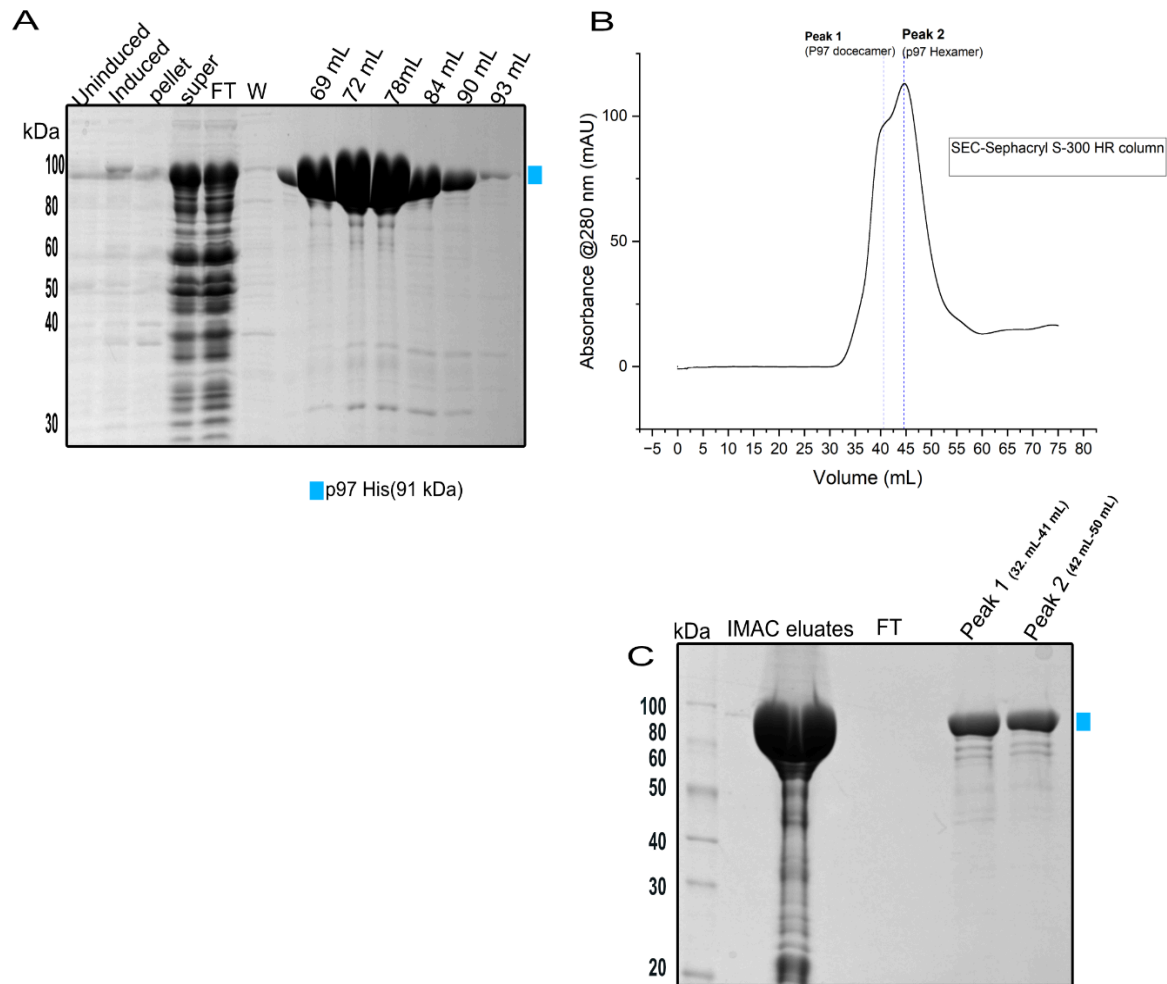


**Figure 3.4 IMAC and SEC purification of the ATPase p97.** 10% glycine SDS-PAGE (reducing condition) analysis of p97 His purification. (A) p97 His was purified using IMAC to separate the protein from cell lysates. (B) The elution profile of p97 His from the SEC (Sephacryl S-300 HR) column (35 mL to 50 mL) revealed distinct peaks corresponding to p97 dodecamer and hexamer. The p97 dodecamer exhibited an earlier peak elution at 40 mL, while the p97 hexamer fragment showed a peak elution at 45 mL. (C) 10% glycine SDS-PAGE (reducing condition) analysis of the peak elution confirms p97 His in these fractions.

### **3.2.3 Purification of Selenoprotein S**

Selenos is one of the selenok's binding partners and selenok has shown to associate with p97 by interacting with selenos [7]. It is predicted by AlphaFold2 [14] to contain three helices: helix 1 (from residues 1-33), helix 2 (residues 34-70), and helix 3 (residues 73-123). The third helix is followed by a C-terminal disordered region 123-189 containing Sec at residue 188. Here, I describe the purification of residues 123-189 of selenos.

Selenos 123-189 was expressed as a MBP fusion protein (6x His-tagged MBP TEV strep selenos 123-189 U188C) in *E. coli*, but it was extracted without DDM or other detergents, as the absence of the membrane-interacting region eliminated the risk of aggregation. Following TEV cleavage, strep-tagged selenos 123-189 U188C was subjected to desalting and further purification using cation IEX (SP) chromatography. The resulting protein exhibited a purity exceeding 95%. (see Figure 3.4 A & B)

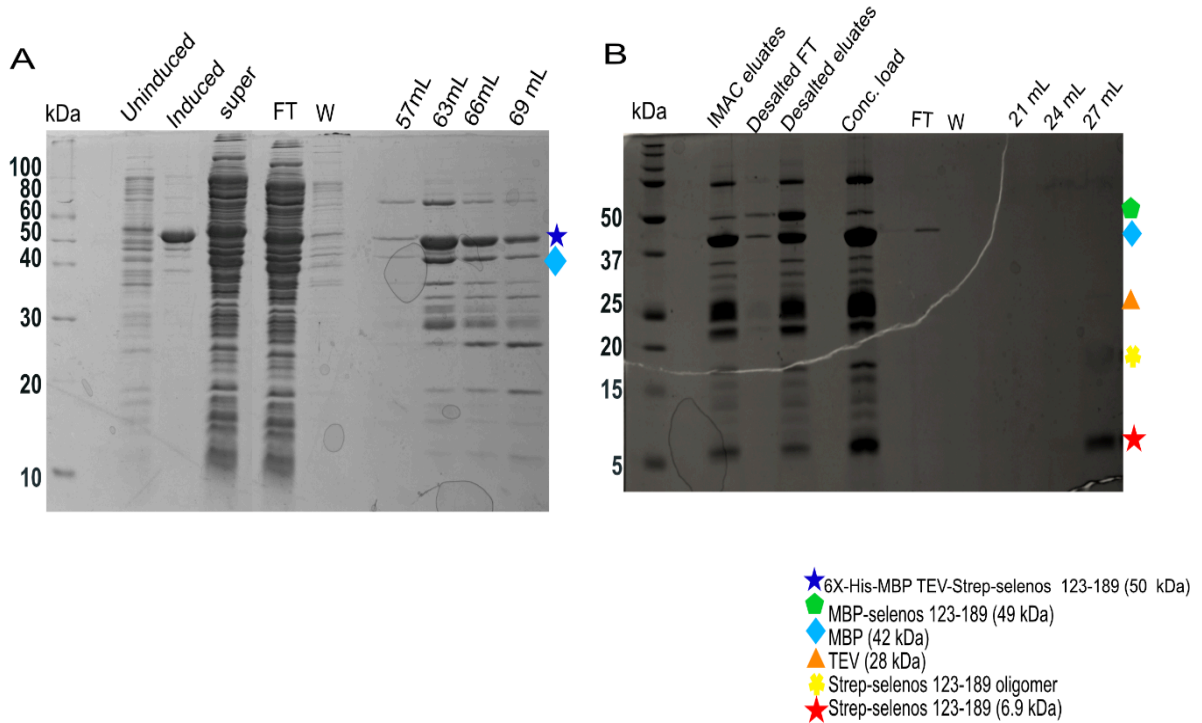


**Figure 3.5: IMAC and cation IEX (SP) chromatography purification of selenos 123-189 U188C.** 16% glycine (A) and 16 % tricine (B) SDS-PAGE (reducing condition) analysis of selenos 123-189 U188C (A) 6x His-MBP-TEV- selenos 123-189 U188C was purified using an IMAC to separate the His-tagged fusion protein from cell lysates (B) IMAC eluates were desalted, incubated with TEV protease, and subsequently purified using cation IEX chromatography to isolate the strep-tagged selenok selenos 123-189 U188C from the TEV protease and MBP.

### 3.4 Discussion

The ERAD machinery plays a crucial role in eliminating misfolded proteins by transporting them from the ER to the cytosol for degradation via the proteasome [1], [3]. Acting as the primary retro-translocation protein, the cytosolic AAA+ ATPase p97 provides the mechanical force necessary for this process [16],[17]. Structurally, p97 comprises four domains: N-terminal, D1, D2, and C-terminal, each fulfilling distinct roles in ERAD [16], [18]. The N-terminal domain is pivotal for recognizing and binding client proteins, as well as interacting with adapters. Similarly, the short C-terminus also serves as a site for adapter binding [19],[20]. The D1 and D2 domains work together to unfold the client proteins, with the D1 domain primarily responsible for nucleotide binding independent of oligomerization. P97 functions as a hexamer, and its crucial activity hinges on conformational changes driven by ATP hydrolysis within the hexameric ring [19], [20].

The cellular functions of p97 are diverse, spanning from ERAD to the regulation of protein complexes and transcriptional control [20]. These functions are influenced by interactions with various partner proteins, particularly those binding to its N-domain [19]. These partners encompass a range of proteins, including E3 ligases such as Hrd1 and grp78, deubiquitinases like ataxn3 and YOD1, and ERAD accessory factors such as UbxD2 and selenos [20], [21], [22], [23]. Previous research has characterized the interaction between p97 and selenos, revealing that selenos directly recruits p97 to the ER through its VIM domain [24]. Within the VIM domain in selenos, 40 residues (A69-E108) are minimally required for p97(VCP) binding [25], [26]. Selenok has also been shown to interact with

multiple proteins in the ERAD pathway, such as derlins, selenos, and the ATPase p97 [6]. Another study suggests that selenok interacts with the p97-selenos complex through its association with selenos [7]. However, the atomic-level details of these interactions, as well as selenok's precise role in ERAD, remain incompletely understood.

A key method for studying membrane protein complexes is by structural studies, such as cryo-EM, as it offers detailed insights into their molecular structure and interactions at an atomic level [11], [12]. Various other methods can be employed to study selenok's function and interaction with protein partners in ERAD. Binding assays, such as immunoprecipitation, affinity pull-downs, and protein-protein interaction studies, help identify interaction partners [27],[28]. Cellular imaging techniques, like immunofluorescence microscopy [29], [30], enable visualization of membrane protein localization and dynamics. Pharmacological strategies utilizing small molecule inhibitors or activators can be used for functional elucidation [31], [32]. Gene knockout and overexpression studies can assess selenok's effects on its ERAD partners when the genes encoding it are silenced or increased [33], [34]. Additionally, proteolytic assays can provide information on its regulatory and enzymatic activity [35], [36].

Many of these methods used to study these interactions require the extraction and purification of these proteins. In this study, we purified selenok's membrane portion (selenok 2-42) as well as its IDR (selenok 43-94). Selenok 2-42 was extracted and purified by IMAC and on a Strep-Tactin XL 4Flow resin in the presence of detergent to prevent aggregation post-purification [15]. Selenok 43-94 was purified by IMAC and IEX (SP)

chromatography without detergent, as the absence of the membrane-interacting region eliminated the risk of aggregation.

We also purified selenok's other ERAD partners, p97 ATPase and selenos. p97 was purified by IMAC and SEC. From the SEC elution peaks, p97 mainly existed as a hexamer but also as a dodecamer. Selenos 123-189 U188C, which is the IDR region of selenos, was purified by IMAC and IEX (SP) chromatography. All proteins showed high purity of at least 90%.

This work lays the foundation for the structural characterization of the selenos-p97 ATPase-selenok complex via cryo-EM and for other future investigative studies into the interaction between selenok and its partners (selenos and p97) with the goal of elucidating selenok's role in the ERAD pathway.

### 3.5 Methods

#### 3.5.1 Expression and purification of selenok (2-43 & 43-94 U92C) selenos (1-123 U188C) and p97 (p97 His)

Expression vector ID	Constructs
SR-10-168	His-MBP-TEV-selenok 2-42
SR-10-161	His-MBP-TEV-selenok 43-94 U92C
SR-60-018	His-MBP-TEV-selenos 123-189 U188C
SR-90-213	P97-His

**Table 3.1: The vector numbers and their corresponding construct**

##### 3.5.1.1 Expression, Harvest, and Lysis

All selenok and selenos constructs were expressed in BL21 (DE3) while p97 was grown in Rosetta (DE3) cells. For the seeding culture, cells were grown in LB media (1 % (w/v) tryptone, 0.5 % (w/v) yeast extract, 0.5 % (w/v) NaCl), selenok and selenos construct were supplemented with 100 µg/ml ampicillin while p97 was supplemented with 50 µg/ml kanamycin and 25 µg/ml chloramphenicol at 37°C while shaking at 200 rpm overnight. To scale up cell culture, the overnight culture was transferred (using ratio 1:100) into 1 L TB media (1.2 % (w/v) tryptone, 2.4 % (w/v) yeast extract, 0.4 % (v/v) glycerol, 2 mM MgSO<sub>4</sub> (2 mM), 0.5% lactose (29.2 mM), 0.015% glucose (1.67 mM), 0.375% neutralized aspartic acid, 17 mM sodium phosphate monobasic, 72 mM sodium phosphate dibasic) supplemented with 100 µg/mL ampicillin for selenok and selenos constructs while p97

received 50 µg/ml kanamycin and 25 µg/ml chloramphenicol. Flasks were grown at 37 °C with 180 rpm shaking. When OD600 of 0.2, the incubator temperature was changed to 18 °C.

After 20 hours of protein expression, cell pellets were harvested by centrifugation at 5,000 g for 30 minutes at 4°C. The harvested pellets were immediately resuspended in cold lysis buffer (50 mM sodium phosphate, 25 mM imidazole, 200 mM NaCl, 1 mM EDTA, pH 7.5) and flash frozen before storage at -80°C. Upon thawing, the cell pellets were lysed using an LM10 microfluidizer after adjusting the cell weight percentage to 15% with lysis buffer supplemented with 0.2% triton X-100 (only for selenok 2-42). Proteins were separated from cell debris by centrifugation at 30,000 g for 60 minutes at 4°C.

The resulting supernatant was purified by loading onto a recharged and equilibrated His-Trap HP IMAC column, followed by washing with wash buffer (50 mM sodium phosphate, 25 mM imidazole, 200 mM NaCl, 1 mM EDTA, 0.2% triton X-100 for selenok 2-42, pH 7.5) and elution with elution buffer (50 mM sodium phosphate, 1 M imidazole, 200 mM NaCl, 0.2% triton X-100 for selenok 2-42, pH 7.5) using a linear gradient. The purity of the recombinant proteins was assessed using SDS-PAGE. To remove the His-MBP tag, the eluate from the IMAC column was desalted into TEV protease cleavage buffer (50 mM sodium phosphate, 25 mM imidazole, 200 mM NaCl, 1 mM EDTA, 0.2% triton X-100 for selenok 2-42, pH 7.5) using a HiPrep 26/10 Desalting column. After desalting, TEV protease was added at a molar ratio of 1:10 for protease to selenok and selenos, and the cleavage cocktail was supplemented with 1 mM DTT and 10% glycerol

before overnight incubation at 4°C. The protein was then spun down to remove any aggregation.

#### **3.5.1.2 Strep-Tactin Purification:**

The TEV-cleaved strep selenok was separated from the tagged MBP, TEV, and other impurities by loading onto pre-equilibrated (50 mM Na<sub>2</sub>HPO<sub>4</sub>, pH 7.5, 200 mM NaCl, 1mM EDTA) Strep-Tactin XT 4Flow resin, followed by washing with the same buffer and elution with the same buffer containing 50 mM biotin.

#### **3.5.1.3 Cation Exchange (SP) Chromatography**

Selenok 43-94 and selenos 123-189 were separated from the tagged MBP, TEV, and other impurities by loading onto a 5 mL HiTrap (SP) column pre-equilibrated with 20 mM bicine, 100 mM NaCl, pH 8.2, and eluted with 20 mM bicine, 1 M NaCl, pH 8.2. p97 was further purified by size exclusion chromatography.

#### **3.5.1.4 Size Exclusion Chromatography**

Size exclusion chromatography was used to refine the purification of p97. A Sephacryl S-300 HR column was equilibrated with 20 mM HEPES, 150 mM NaCl, 1 mM TCEP pH 7.5 at a flow rate of 0.2 mL/min. Protein concentration was done using anAmicon Ultra-15 Centrifugal Filters with a 30 kDa cutoff. p97 His was concentrated to 12 mg/ml, and 3 mL of protein solution was loaded onto the column and run at a flow rate of 0.2 mL/min.

### **3.5.2 Tricine SDS-PAGE Analysis**

SDS-PAGE analysis was conducted to evaluate protein purity. Protein samples were mixed with 4X glycine or tricine loading buffer containing 1% 2-mercapthoethanol (reducing agent). Subsequently, 6  $\mu$ L of the sample was loaded onto a 16% tricine gel or 16% glycine gel and electrophoresed at 90 V for 20 minutes, then increasing to 170 V for 40 minutes. For gel imaging, only the tricine gel was fixed in a solution of 50% methanol, 10% acetic acid, and 100 mM ammonium acetate for 15 minutes. Both gels were stained with Coomassie for 45 minutes and destained in 10% acetic acid

## REFERENCES

- [1] Krshnan, L et al. "Endoplasmic reticulum–associated protein degradation." Cold Spring Harbor Perspectives in Biology 14.12 (2022): a041247.
- [2] Tomohiro Omura et al. "Endoplasmic Reticulum Stress and Parkinson's Disease: The Role of HRD1 in Averting Apoptosis in Neurodegenerative Disease" Oxidative Medicine and Cellular Longevity, 2013. Volume 2013 | Article ID 239854 |<https://doi.org/10.1155/2013/239854>
- [3] Qi, L., Tsai, B. and Arvan, P. "New insights into the physiological role of endoplasmic reticulum-associated degradation". Trends Cell Biol. 27, 430-440. <https://doi.org/10.1016/j.tcb.2016.12.002>
- [4] Lemberg, Marius K., and Kvido Strisovsky. "Maintenance of organellar protein homeostasis by ER-associated degradation and related mechanisms." Molecular Cell 81.12 (2021): 2507-2519.
- [5] Lemberg, Marius K., and Kvido Strisovsky. "Maintenance of organellar protein homeostasis by ER-associated degradation and related mechanisms." Molecular Cell 81.12 (2021): 2507-2519.
- [6]. Kang, Ji An, and Young Joo Jeon. "How is the fidelity of proteins ensured in terms of both quality and quantity at the endoplasmic reticulum? Mechanistic

insights into E3 ubiquitin ligases." *International Journal of Molecular Sciences* 22.4 (2021): 2078.

[7] V. A. Shchedrina, R. A. Everley, Y. Zhang, S. P. Gygi, D. L. Hatfield, and V. N. Gladyshev, "Selenoprotein K Binds Multiprotein Complexes and Is Involved in the Regulation of Endoplasmic Reticulum Homeostasis \*," *J. Biol. Chem.*, vol. 286, no. 50, pp. 42937–42948, Dec. 2011, doi: 10.1074/JBC.M111.310920

[8] Ye, Y., et al. "Inaugural article: recruitment of the p97 ATPase and ubiquitin ligases to the site of retrotranslocation at the endoplasmic reticulum membrane". *Proc. Natl. Acad. Sci. U. S. A.* 2005 102:14132–14138.

[9] J. H. Lee et al., "Selenoprotein S-dependent selenoprotein K binding to p97(VCP) protein is essential for endoplasmic reticulum-associated degradation," *J. Biol. Chem.*, vol. 290, no. 50, pp. 29941–29952, 2015, doi: 10.1074/jbc.M115.680215

[10] E. P. Carpenter, K. Beis, A. D. Cameron, and S. Iwata, "Overcoming the challenges of membrane protein crystallography," *Current Opinion in Structural Biology*, vol. 18, no. 5, pp. 581–586, Oct. 2008, doi: 10.1016/j.sbi.2008.07.001.

[11] Cheng, Yifan. "Membrane protein structural biology in the era of single particle cryo-EM." *Current opinion in structural biology* 52 (2018): 58-63.

[12] Yao, Xia, Xiao Fan, and Nieng Yan. "Cryo-EM analysis of a membrane protein embedded in the liposome." *Proceedings of the National Academy of Sciences* 117.31 (2020): 18497-18503.

- [13] Radermacher, Michael, et al. "Cryo-electron microscopy and three-dimensional reconstruction of the calcium release channel/ryanodine receptor from skeletal muscle." *The Journal of cell biology* 127.2 (1994): 411-423.
- [14] J. Jumper et al., "Highly accurate protein structure prediction with AlphaFold," *Nature*, vol. 596, no. 7873, pp. 583–589, Aug. 2021, doi: 10.1038/s41586-021-03819-2.
- [15] Liu, Jun, et al. "Expression and purification of the membrane enzyme selenoprotein K." *Protein expression and purification* 86.1 (2012): 27-34.
- [16] Segura-Cabrera, Aldo, et al. "A structure-and chemical genomics-based approach for repositioning of drugs against VCP/p97 ATPase." *Scientific reports* 7.1 (2017): 44912.
- [17] Lim, Jia Jia, et al. "Structural insights into the interaction of human p97 N-terminal domain and SHP motif in Derlin-1 rhomboid pseudoprotease." *FEBS letters* 590.23 (2016): 4402-4413.
- [18] X. Wu and T. A. Rapoport, "Mechanistic insights into ER-associated protein degradation," *Current Opinion in Cell Biology*, vol. 53, pp. 22–28, Aug. 2018, doi: 10.1016/j.ceb.2018.04.004.
- [19] Braxton JR, Southworth DR. "Structural insights of the p97/VCP AAA+ ATPase: How adapter interactions coordinate diverse cellular functionality". *J Biol Chem*. 2023 Nov;299(11):105182. doi: 10.1016/j.jbc.2023.105182
- [20] Tepedelen, Burcu Erbaykent, and Petek Ballar Kirmizibayrak. "Endoplasmic reticulum-associated degradation (ERAD)." *Endoplasmic Reticulum* (2019).
- [21] Lopata, Anna, et al. "Ubiquitination in the ERAD Process." *International journal of molecular sciences* 21.15 (2020): 5369.

- [22] Sasset, Linda, et al. "The VCP/p97 and YOD1 proteins have different substrate-dependent activities in endoplasmic reticulum-associated degradation (ERAD)." *Journal of Biological Chemistry* 290.47 (2015): 28175-28188.
- [23] Papadopoulos, Chrisovalantis, et al. "VCP/p97 cooperates with YOD 1, UBXD 1 and PLAA to drive clearance of ruptured lysosomes by autophagy." *The EMBO journal* 36.2 (2017): 135-150.
- [24] W. K. Tang, T. Zhang, Y. Ye, and D. Xia, "Structural basis for nucleotide modulated p97 association with the ER membrane," *Cell Discov*, vol. 3, no. 1, p. 17045, Dec. 2017, doi: 10.1038/celldisc.2017.45.
- [25] F. Ghelichkhani et al., "Selenoprotein S: A versatile disordered protein," *Archives of Biochemistry and Biophysics*, vol. 731, p. 109427, Nov. 2022, doi: 10.1016/j.abb.2022.109427.
- [26] J. H. Lee et al., "Selenoprotein S-dependent selenoprotein K binding to p97(VCP) protein is essential for endoplasmic reticulum-associated degradation," *J. Biol. Chem.*
- [27] Parra-Belky, Karlett, et al. "Immunoprecipitation and characterization of membrane protein complexes from yeast\* S." *Biochemistry and Molecular Biology Education* 33.4 (2005): 289-292.
- [28] Avila, Julian R., Jin Suk Lee, and Keiko U. Torii. "Co-immunoprecipitation of membrane-bound receptors." *The Arabidopsis book/American society of plant biologists* 13 (2015).

- [29] Wang, Chao, et al. "Immunofluorescence analysis of membrane-associated proteins for clathrin-mediated endocytosis in plant root cells." *Plant Protein Secretion: Methods and Protocols* (2017): 151-157.
- [30] Roux, Kyle J., et al. "Nesprin 4 is an outer nuclear membrane protein that can induce kinesin-mediated cell polarization." *Proceedings of the National Academy of Sciences* 106.7 (2009): 2194-2199.
- [31] Sheng, Chunquan, et al. "State-of-the-art strategies for targeting protein–protein interactions by small-molecule inhibitors." *Chemical Society Reviews* 44.22 (2015): 8238-8259.
- [32] Yin, Hang, and Aaron D. Flynn. "Drugging membrane protein interactions." *Annual review of biomedical engineering* 18 (2016): 51-76.
- [33] Qiu, Zhaozhu, et al. "SWELL1, a plasma membrane protein, is an essential component of volume-regulated anion channel." *Cell* 157.2 (2014): 447-458.
- [34] Gao, Fang, et al. "Novel binding between pre-membrane protein and claudin-1 is required for efficient dengue virus entry." *Biochemical and biophysical research communications* 391.1 (2010): 952-957.
- [35] Lichtenthaler, Stefan F., Marius K. Lemberg, and Regina Fluhrer. "Proteolytic ectodomain shedding of membrane proteins in mammals—hardware, concepts, and recent developments." *The EMBO journal* 37.15 (2018): e99456.
- [36] Besingi, Richard N., and Patricia L. Clark. "Extracellular protease digestion to evaluate membrane protein cell surface localization." *Nature protocols* 10.12 (2015): 2074.